siveness. *Am J Physiol* 1993; **264**: C1367–C1387.
6. Blaustein MP: Endogenous ouabain: role in the pathogenesis of hypertension. *Kidney Int* 1996; **49**: 1748–1753.
7. Nelson LD, Unlap MT, Lewis JL, Bell PD: Renal arteriolar Na^+/Ca^{2+} exchange in salt-sensitive hypertension. *Am J Physiol* 1999; **276**: F567–F573.
8. Nelson LD, Mashburn NA, Bell PD: Altered sodium-calcium exchange in afferent arterioles of the spontaneously hypertensive rat. *Kidney Int* 1996; **50**: 1889–1896.
9. Unlap MT, Peti-Peterdi J, Bell PD: Cloning of mesangial cell Na^+/Ca^{2+} exchangers from Dahl/Rapp salt-sensitive/resistant rats. *Am J Physiol Renal Physiol* 2000; **279**: F177–F184.
10. Ashida T, Kuramochi M, Omae T: Increased sodium-calcium exchange in arterial smooth muscle of spontaneously hypertensive rats. *Hypertension* 1989; **13**: 890–895.
11. Ashida T, Kawano Y, Yoshimi H, Kuramochi M, Omae T: Effects of dietary salt on sodium-calcium exchange and ATP-driven calcium pump in arterial smooth muscle of Dahl rats. *J Hypertens* 1992; **10**: 1335–1341.
12. Kraev A, Chumakov I, Carafoli E: The organization of the human gene *NCX1* encoding the sodium-calcium exchanger. *Genomics* 1996; **37**: 105–112.
13. Kofuji P, Lederer WJ, Schulze DH: Mutually exclusive and cassette exons underlie alternatively spliced isoforms of the Na/Ca exchanger. *J Biol Chem* 1994; **269**: 5145–5149.
14. Barnes KV, Cheng G, Dawson MM, Menick DR: Cloning of cardiac, kidney, and brain promoters of the feline *NCX1* gene. *J Biol Chem* 1997; **272**: 11510–11517.
15. Lee SL, Yu AS, Lytton J: Tissue-specific expression of Na^+-Ca^{2+} exchanger isoforms. *J Biol Chem* 1994; **269**: 14849–14852.
16. Nicholas SB, Yang W, Lee SL, Zhu H, Philipson KD, Lytton J: Alternative promoters and cardiac muscle cell-specific expression of the Na^+/Ca^{2+} exchanger gene. *Am J Physiol* 1998; **274**: H217–H232.
17. Scheller T, Kraev A, Skinner S, Carafoli E: Cloning of the multipartite promoter of the sodium-calcium exchanger gene *NCX1* and characterization of its activity in vascular smooth muscle cells. *J Biol Chem* 1998; **273**: 7643–7649.
18. Joint National Committee on Prevention, Detection, Evaluation, and Treatment of High Blood Pressure: The sixth report of the Joint National Committee on Prevention, Detection, Evaluation, and Treatment of High Blood Pressure. *Arch Intern Med* 1997; **157**: 2413–2446.
19. Kamide K, Tanaka C, Takiuchi S, *et al*: Six missense mutations of the epithelial sodium channel β and γ subunits in Japanese hypertensives. *Hypertens Res* 2004; 333–338.
20. Tanaka C, Kamide K, Takiuchi S, *et al*: An alternative fast and convenient genotyping method for the screening of angiotensin converting enzyme gene polymorphisms. *Hypertens Res* 2003; **26**: 301–306.
21. Inamoto N, Katsuya T, Kokubo Y, *et al*: Association of methylenetetrahydrofolate reductase gene polymorphism with carotid atherosclerosis depending on smoking status in a Japanese general population. *Stroke* 2003; **34**: 1628–1633.
22. Hwang EF, Williams I, Kovacs G, *et al*: Impaired ability of the Na^+/Ca^{2+} exchanger from the Dahl/Rapp salt-sensitive rat to regulate cytosolic calcium. *Am J Physiol Renal Physiol* 2003; **284**: F1023–F1031.
23. Meade TW, Imeson JD, Gordon D, Peart WS: The epidemiology of plasma renin. *Clin Sci* (*Lond*) 1983; **64**: 273–280.
24. Alderman MH, Madhavan S, Cohen H, Sealey JE, Laragh JH: Low urinary sodium is associated with greater risk of myocardial infarction among treated hypertensive men. *Hypertension* 1995; **25**: 1144–1152.
25. Furman I, Cook O, Kasir J, Low W, Rahamimoff H: The putative amino-terminal signal peptide of the cloned rat brain Na^+-Ca^{2+} exchanger gene (RBE-1) is not mandatory for functional expression. *J Biol Chem* 1995; **270**: 19120–19127.
26. Loo TW, Ho C, Clarke DM: Expression of a functionally active human renal sodium-calcium exchanger lacking a signal sequence. *J Biol Chem* 1995; **270**: 19345–19350.

Am J Physiol Heart Circ Physiol 287: H2670–H2676, 2004.
First published July 29, 2004; doi:10.1152/ajpheart.01071.2003

Intravenous administration of mesenchymal stem cells improves cardiac function in rats with acute myocardial infarction through angiogenesis and myogenesis

Noritoshi Nagaya,[1,2] Takafumi Fujii,[3] Takashi Iwase,[1] Hajime Ohgushi,[4] Takefumi Itoh,[1] Masaaki Uematsu,[5] Masakazu Yamagishi,[2] Hidezo Mori,[3] Kenji Kangawa,[6] and Soichiro Kitamura[7]

Departments of [1]Regenerative Medicine and Tissue Engineering, [3]Cardiac Physiology, and [6]Biochemistry, National Cardiovascular Center Research Institute, Osaka 565-8565; Departments of [2]Internal Medicine and [7]Cardiovascular Surgery, National Cardiovascular Center, Osaka; [4]Tissue Engineering Research Center, National Institute of Advanced Industrial Science and Technology, Hyogo; and [5]Cardiovascular Division, Kansai Rosai Hospital, Hyogo 660-8511, Japan

Submitted 10 November 2003; accepted in final form 13 July 2004

Nagaya, Noritoshi, Takafumi Fujii, Takashi Iwase, Hajime Ohgushi, Takefumi Itoh, Masaaki Uematsu, Masakazu Yamagishi, Hidezo Mori, Kenji Kangawa, and Soichiro Kitamura. Intravenous administration of mesenchymal stem cells improves cardiac function in rats with acute myocardial infarction through angiogenesis and myogenesis. *Am J Physiol Heart Circ Physiol* 287: H2670–H2676, 2004. First published July 29, 2004; doi:10.1152/ajpheart.01071.2003.—Mesenchymal stem cells (MSCs) are pluripotent cells that differentiate into a variety of cells, including cardiomyocytes and endothelial cells. However, little information is available regarding the therapeutic potency of systemically delivered MSCs for myocardial infarction. Accordingly, we investigated whether intravenously transplanted MSCs induce angiogenesis and myogenesis and improve cardiac function in rats with acute myocardial infarction. MSCs were isolated from bone marrow aspirates of isogenic adult rats and expanded ex vivo. At 3 h after coronary ligation, 5×10^6 MSCs (MSC group, $n = 12$) or vehicle (control group, $n = 12$) was intravenously administered to Lewis rats. Transplanted MSCs were preferentially attracted to the infarcted, but not the noninfarcted, myocardium. The engrafted MSCs were positive for cardiac markers: desmin, cardiac troponin T, and connexin43. On the other hand, some of the transplanted MSCs were positive for von Willebrand factor and formed vascular structures. Capillary density was markedly increased after MSC transplantation. Cardiac infarct size was significantly smaller in the MSC than in the control group (24 ± 2 vs. 33 ± 2%, $P < 0.05$). MSC transplantation decreased left ventricular end-diastolic pressure and increased left ventricular maximum dP/dt (both $P < 0.05$ vs. control). These results suggest that intravenous administration of MSCs improves cardiac function after acute myocardial infarction through enhancement of angiogenesis and myogenesis in the ischemic myocardium.

left ventricular end-diastolic pressure; cell transplantation; differentiation; homing

INTERRUPTION OF MYOCARDIAL blood flow leads to cardiomyocyte death (20). Although myocyte mitosis and the presence of cardiac precursor cells in adult hearts have recently been reported (6, 17), death of large numbers of cardiomyocytes results in the development of heart failure (16). Thus it would be desirable to induce angiogenesis and myogenesis for the treatment of ischemic heart disease.

Mesenchymal stem cells (MSCs) are pluripotent adult stem cells residing within the bone marrow microenvironment (11, 18). In contrast to their hematopoietic counterparts, MSCs have an adherent nature and are expandable in culture. MSCs can differentiate into not only osteoblasts, chondrocytes, neurons, and skeletal muscle cells but also vascular endothelial cells (19) and cardiomyocytes (23, 24). In vitro, MSCs have the potential to induce a neovascular response in murine Matrigel angiogenesis assay (2). In vivo, local MSC implantation induces therapeutic angiogenesis in a rat model of hindlimb ischemia (1). On the other hand, MSCs directly injected into the infarcted heart have been shown to induce myocardial regeneration and improve cardiac function (21). Stem or progenitor cells have been shown to circulate in peripheral blood and home to ischemic tissues (4). These results raise the possibility that intravenously administered MSCs participate in repair of the ischemic myocardium primarily by angiogenesis, which prevents apoptosis of native cardiomyocytes, and by direct regeneration of lost cardiomyocytes. However, little information is available regarding the therapeutic potential of systemically delivered MSCs for myocardial infarction.

Thus the purpose of this study was to investigate whether *1*) intravenously administered MSCs are able to engraft in the ischemic myocardium, *2*) transplanted MSCs induce angiogenesis and myogenesis after myocardial infarction, and *3*) transplantation of MSCs decreases infarct size and improves cardiac function.

METHODS

Animals. Male Lewis rats ($n = 70$) weighing 220–250 g were used in this study. These isogenic rats ($n = 8$) served as donors and recipients of MSCs to simulate autologous implantation. The Animal Care Committee of the National Cardiovascular Center approved the experimental protocol.

Model of myocardial infarction and cell transplantation. Fifty-one rats underwent ligation of the left coronary artery to produce myocardial infarction, as described previously (15). Briefly, after rats were anesthetized by injection of pentobarbital sodium (30 mg/kg body wt ip), they were artificially ventilated using a volume-regulated respirator. The heart was exposed via a left thoracotomy, and the left coronary artery was ligated 2–3 mm from its origin between the pulmonary artery conus and the left atrium using a 6-0 Prolene suture.

Address for reprint requests and other correspondence: N. Nagaya, Dept. of Regenerative Medicine and Tissue Engineering, National Cardiovascular Center Research Institute, 5-7-1 Fujishirodai, Suita, Osaka 565-8565, Japan (E-mail: nnagaya@ri.ncvc.go.jp).

The costs of publication of this article were defrayed in part by the payment of page charges. The article must therefore be hereby marked "*advertisement*" in accordance with 18 U.S.C. Section 1734 solely to indicate this fact.

At 3 h after coronary ligation, 40 rats survived (78% survival rate): 30 were randomized to receive an intravenous injection of MSCs (MSC group, $n = 14$) or PBS (control group, $n = 16$), and 10 received fluorescence-labeled MSCs for examination of MSC differentiation ($n = 5$) and incorporation ($n = 5$). Eleven rats underwent a sham operation consisting of thoracotomy and cardiac exposure but without coronary artery ligation. At 3 h after coronary ligation, we administered 5×10^6 MSCs/100 μl in PBS or PBS alone through a catheter inserted into the left jugular vein in ~30 s. The subsequent mortality for 4 wk was 25% in the control group and 14% in the MSC group. This protocol resulted in the creation of three groups: normal rats given PBS (sham group, $n = 11$), myocardial infarction rats given PBS (control group, $n = 12$), and myocardial infarction rats given MSCs (MSC group, $n = 12$).

Expansion of bone marrow MSCs. MSC expansion was performed according to previously described methods (18). Briefly, we killed the male Lewis rats and harvested the bone marrow by flushing the cavity of the femurs and tibias with PBS. Bone marrow cells were introduced into 100-mm dishes and cultured in α-MEM supplemented with 10% FBS and antibiotics. A small number of cells developed visible symmetrical colonies by *day 5–7*. Nonadherent hematopoietic cells were removed, and the medium was replaced. The adherent, spindle-shaped MSC population expanded to $>5 \times 10^7$ cells by approximately four to five passages after the cells were first cultured.

Flow cytometry. Adherent cells were analyzed by fluorescence-activated cell sorting (FACS SCAN flow cytometer, Becton Dickinson). Cells were incubated for 30 min at 4°C with the FITC-conjugated mouse monoclonal antibodies against rat CD34 (clone ICO-115, Santa Cruz Biotechnology) and CD45 and CD90 (clones OX-1 and OX-7, respectively, Becton Dickinson). FITC-conjugated hamster anti-rat CD29 monoclonal antibody (clone Ha2/5, Becton Dickinson) and rabbit anti-rat c-Kit polyclonal antibody (clone C-19, Santa Cruz Biotechnology) were used. Isotype-identical antibodies served as controls.

Echocardiographic studies. Echocardiographic studies were performed by an investigator blinded to treatment allocation 4 wk after coronary ligation. Two-dimensional targeted M-mode traces were obtained at the level of the papillary muscles using an echocardiographic system equipped with a 7.5-MHz phased-array transducer (SONOS 5500, Hewlett-Packard, Andover, MA). Anterior and posterior end-diastolic wall thickness and left ventricular (LV) end-diastolic and end-systolic dimensions were measured by the American Society for Echocardiology leading-edge method from at least three consecutive cardiac cycles. LV fractional shortening was calculated as follows: $(LVD_d - LVD_s)/LVD_d \times 100$, where LVD_d is LV diastolic dimension and LVD_s is LV systolic dimension. LV volume and ejection fraction were calculated on the basis of the Teichholtz formula.

Hemodynamic studies. Hemodynamic studies were performed 4 wk after coronary ligation. A 1.5-Fr micromanometer-tipped catheter (Millar Instruments) was inserted in the right carotid artery for measurement of mean arterial pressure. Then the catheter was advanced into the LV for measurement of LV pressure. Hemodynamic variables were measured using a pressure transducer (model P23 ID, Gould) connected to a polygraph. After completion of these measurements, the left and right ventricles were excised and weighed. Infarction size was determined as a percentage of the entire LV area, as reported previously (8). Briefly, incisions were made in the LV, so that the tissue could be pressed flat. The circumference of the entire flat LV and the visualized infarcted area, as judged from the epicardial and endocardial sides, was outlined on a clear plastic sheet. The difference in weight between the two marked areas on the sheet was used to determine infarction size and was expressed as a percentage of LV surface area.

Histological examination. To detect fibrosis in cardiac muscle, the LV myocardium ($n = 5$ each group) was fixed in 10% formalin, cut transversely, embedded in paraffin, and stained with Masson's trichrome. To detect capillary endothelial cells in the peri-infarct area, samples of the harvested muscle ($n = 5$ each) were embedded in OCT compound (Miles Scientific), snap frozen in liquid nitrogen, and cut into transverse sections. Tissue sections were stained for alkaline phosphatase with an indoxyltetrazolium method. The number of capillary vessels was counted in the peri-infarct area using a light microscope at ×200 magnification. The numbers in five high-power fields were averaged and expressed as the number of capillary vessels. These morphometric studies were performed by two examiners who were blinded to treatment.

An additional five rats were used to examine whether transplanted MSCs differentiated into cardiomyocytes or vascular endothelial cells. Suspended MSCs were labeled with fluorescent dyes with a PKH-26 red fluorescent cell linker kit (Sigma Chemical, St. Louis, MO) before implantation, as reported previously (13). Fluorescence-labeled MSCs were intravenously administered 3 h after coronary ligation. This subgroup of rats was killed 4 wk after coronary ligation. After the LV was excised and dissected free, muscle samples were embedded in OCT compound, snap frozen in liquid nitrogen, and cut into sections. Immunofluorescent staining for cardiac and endothelial cell markers was performed using monoclonal mouse antidesmin (Dako), anti-cardiac troponin T (Novo), anticonnexin43 (Sigma Chemical), and polyclonal rabbit anti-von Willebrand factor (Dako). FITC-conjugated IgG antibody (BD Pharmingen and Molecular Probes) was used as a secondary antibody.

At 24 h after intravenous administration of PKH-26-labeled MSCs, cardiac muscle was embedded in OCT compound and snap frozen in liquid nitrogen. Then the cardiac muscle from base to apex was

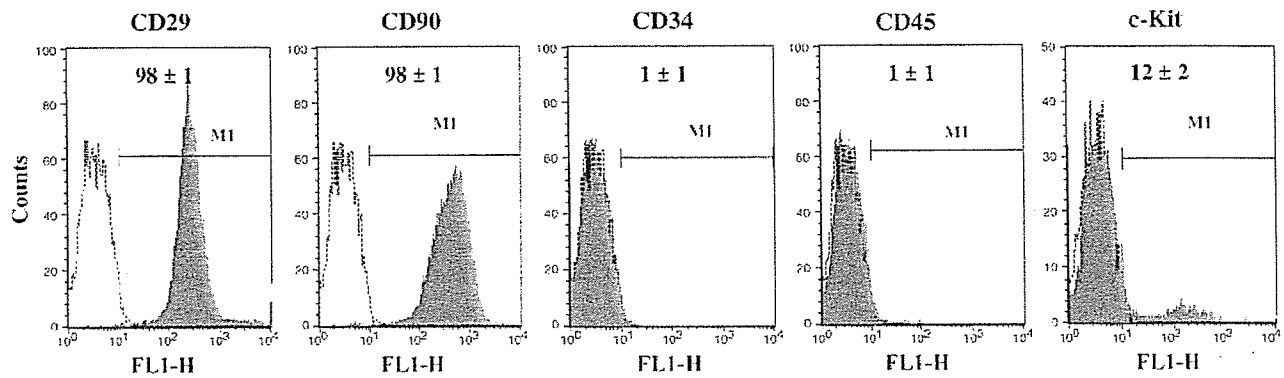

Fig. 1. Flow cytometric analysis of adherent, spindle-shaped mesenchymal stem cell (MSC) population expanded to 4–5 passages. Most of the cells expressed CD29 and CD90 but were negative for CD34 and CD45. Some cells were positive for c-Kit. MI, myocardial infarction.

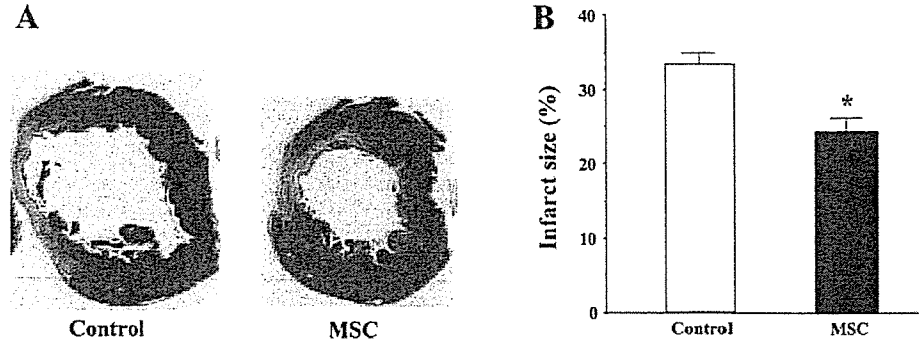

Fig. 2. Effect of MSC transplantation on myocardial infarct size 4 wk after myocardial infarction. *A*: representative Masson's trichrome-stained myocardial sections from control and MSC groups. *B*: quantitative analysis demonstrating that MSC transplantation significantly decreased infarct size. Values are means ± SE. *$P < 0.05$ vs. control.

transversely cut into 5-μm slices for calculation of the numbers of transplanted MSCs in the heart ($n = 5$).

Statistical analysis. Numerical values were expressed as means ± SE unless otherwise indicated. Comparisons of parameters among the three groups were made using one-way analysis of variance (ANOVA) followed by Scheffé's multiple comparison test. Comparisons of parameters between two groups were made by unpaired Student's *t*-test. $P < 0.05$ was considered significant.

RESULTS

Characterization of cultured MSCs. Most of cultured adherent cells expressed CD29 and CD90 (Fig. 1). In contrast, a majority of adherent cells were negative for CD34 and CD45. A small fraction of the adherent cells expressed c-Kit. Thus we confirmed that the major population of adherent cells was MSCs.

Reduction of myocardial infarct size after MSC transplantation. Moderate-to-large infarcts were observed in Masson's trichrome-stained myocardial sections 4 wk after coronary ligation (control group; Fig. 2*A*). However, MSC transplantation markedly decreased the infarct size after myocardial infarction (MSC group). Quantitative analysis also demonstrated that cardiac infarct size was significantly smaller in the MSC than in the control group: 24 ± 2 vs. 33 ± 2% ($n = 12$ each, $P < 0.05$; Fig. 2*B*).

Hemodynamic effects of MSC transplantation. At 4 wk after coronary ligation, hemodynamic studies were performed in the sham ($n = 11$), control ($n = 12$), and MSC ($n = 12$) groups. LV end-diastolic pressure showed a marked elevation in the control group (18 ± 1 mmHg); the elevation was significantly attenuated in the MSC group (13 ± 1 mmHg, $P < 0.05$; Fig. 3*A*). LV maximum dP/d*t* was significantly higher in the MSC than in the control group (Fig. 3*B*). LV minimum dP/d*t* tended to be lower in the MSC than in the control group (Fig. 3*C*). Although mean arterial pressure was significantly lower in the control than in the sham group, no decrease was observed in the MSC group (Table 1). Heart rate did not significantly differ among the three groups.

LV diastolic dimension was significantly smaller in the MSC than in the control group (Table 2). Fractional shortening was significantly greater in the MSC than in the control group (Fig. 3*D*). LV ejection fraction was also higher in the MSC than in

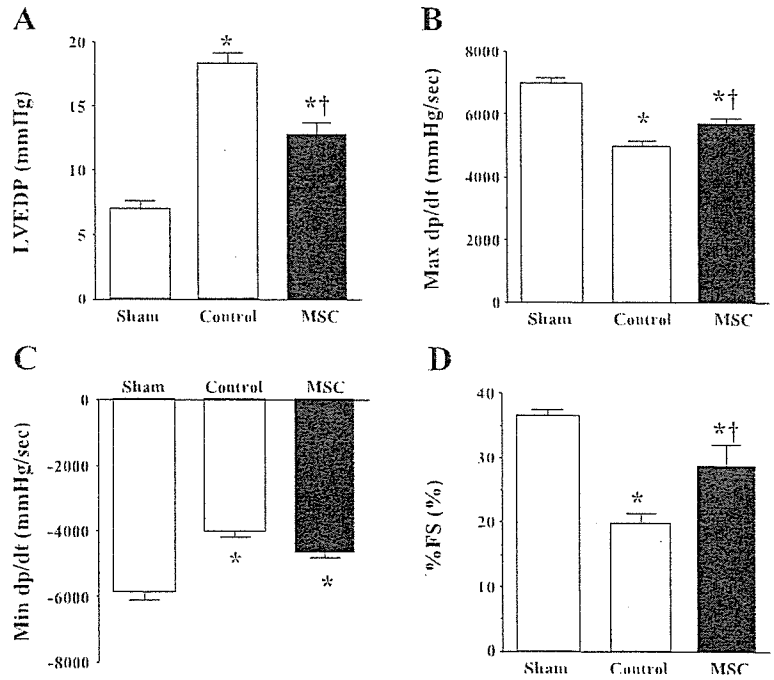

Fig. 3. Effects of MSC transplantation on hemodynamic parameters. LVEDP, LV end-diastolic pressure (*A*); max dP/d*t*, LV maximum dP/d*t* (*B*). Min dP/d*t*, LV minimum dP/d*t* (*C*). %FS, LV fractional shortening (*D*). Values are means ± SE. *$P < 0.05$ vs. sham. †$P < 0.05$ vs. control.

Table 1. *Characterization of animals*

	Sham (n = 11)	Control (n = 12)	MSC (n = 12)
Body wt, g	331±4	301±7*	321±7†
LV wt/body wt, g/kg	1.83±0.11	2.22±0.10*	2.17±0.09*
RV wt/body wt, g/kg	0.55±0.02	0.83±0.04*	0.71±0.03*†
Heart rate, beats/min	404±15	428±17	418±15
Mean arterial pressure, mmHg	128±2	113±4*	119±3

Values are means ± SE. Sham, sham-operated rats given vehicle; control, myocardial infarction rats given vehicle; MSC, myocardial infarction rats given mesenchymal stem cells; LV, left ventricle; RV, right ventricle. *P < 0.05 vs. sham. †P < 0.05 vs. control

Table 2. *Echocardiographic data*

	Sham	Control	MSC
LVD_d, mm	6.3±0.1	8.6±0.2*	7.5±0.3*†
LVD_s, mm	4.0±0.1	6.9±0.3*	5.5±0.5*†
%FS, %	37±1	20±2*	29±3*†
LVEF, %	65±1	39±3*	53±5*†
AWT diastole, mm	1.6±0.1	1.1±0.1*	1.4±0.1†
PWT diastole, mm	1.6±0.1	1.7±0.1	1.7±0.1

Values are means ± SE. LVD_d, LV diastolic dimension; LVD_s, LV systolic dimension; %FS, LV fractional shortening; LVEF, LV ejection fraction; AWT, anterior wall thickness; PWT, posterior wall thickness. *P < 0.05 vs. sham. †P < 0.05 vs. control

the control group (Table 2). Diastolic anterior wall thickness was significantly attenuated in the MSC group compared with the control group.

Myogenesis and angiogenesis induced by MSCs. Red fluorescence-labeled MSCs were intravenously administered 3 h after coronary ligation (n = 5). Semiquantitative analysis demonstrated that ~3% of the transplanted MSCs were incorporated into the heart 24 h after transplantation. At 4 wk after transplantation (n = 5), MSCs were incorporated predominantly into the border zone of infarcts (Fig. 4), whereas few MSCs were detected in the noninfarcted myocardium. Immunofluorescence analyses demonstrated that the engrafted MSCs were positive for desmin (Fig. 4), cardiac troponin T (Fig. 5*A*), and connexin43 (Fig. 5*B*). These results suggest the ability of MSCs to engraft in the ischemic myocardium and differentiate into cardiomyocytes. On the other hand, some of the transplanted MSCs were positive for von Willebrand factor and formed vascular structures (Fig. 6). Alkaline phosphatase staining of the ischemic myocardium showed marked augmentation of neovascularization in the MSC group (Fig. 7*A*). Quantitative analysis demonstrated that capillary density was significantly higher in the MSC than in the control group (n = 5 each; Fig. 7*B*).

DISCUSSION

In the present study, we demonstrated that intravenously administered MSCs were capable of engraftment in the ischemic myocardium and that the engrafted MSCs differentiated into cardiomyocytes and vascular endothelial cells, resulting in myogenesis and angiogenesis. We also demonstrated that MSC transplantation decreased myocardial infarct size and improved cardiac function after acute myocardial infarction in rats.

Earlier studies showed that MSCs directly injected into the myocardium or those injected into coronary arteries improve cardiac function after myocardial infarction. However, little information is available regarding the therapeutic potential of systemically delivered MSCs for myocardial infarction. This study demonstrated that intravenous administration of MSCs

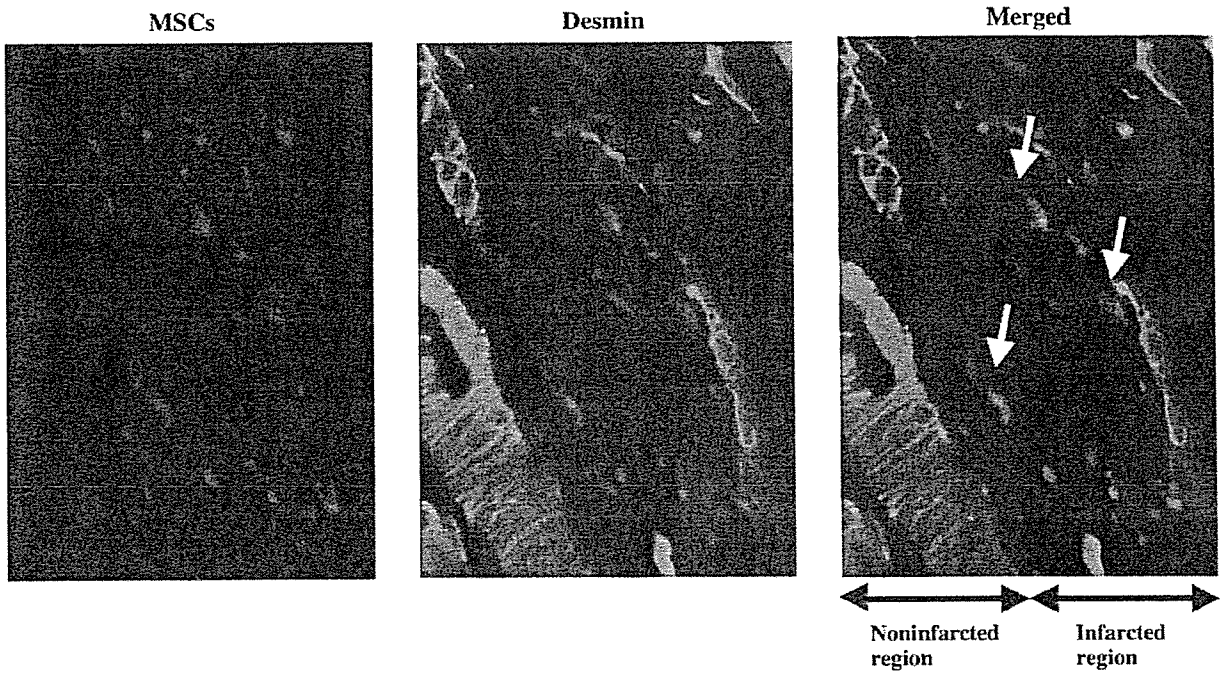

Fig. 4. Distribution of intravenously administered MSCs in myocardium after acute myocardial infarction. Red fluorescence labeled MSCs were incorporated into ischemic boundary zone of the heart. These cells were positive for desmin (arrows), a cardiac marker. Magnification ×400.

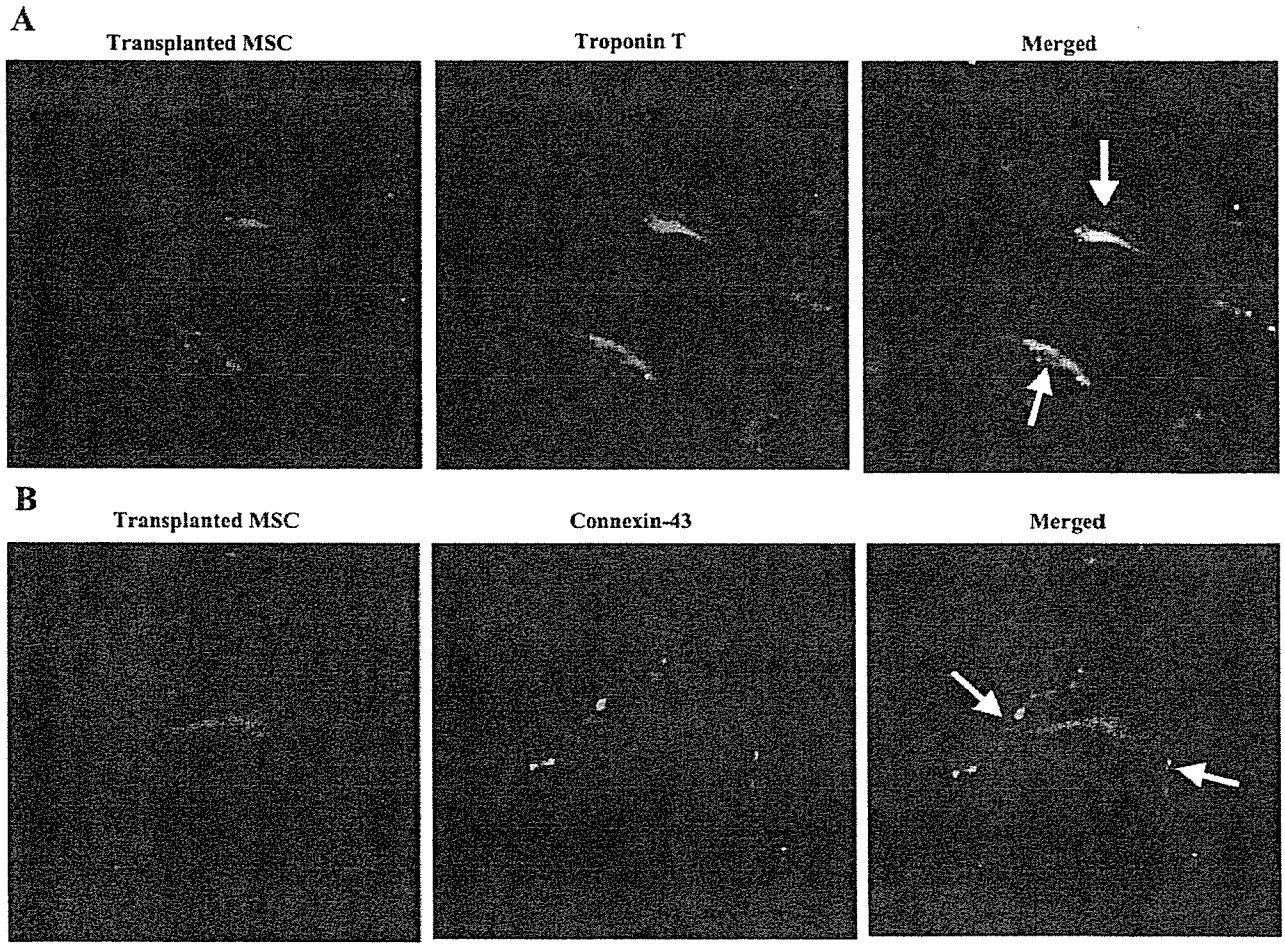

Fig. 5. Differentiation of transplanted MSCs in ischemic myocardium. Engrafted MSCs were positive (arrows) for cardiac troponin T (*A*) and connexin43 (*B*). Magnification ×400.

improves cardiac function after acute myocardial infarction through enhancement of angiogenesis and myogenesis in the ischemic myocardium.

Earlier studies showed that endothelial progenitor cells are mobilized from bone marrow into the peripheral blood in response to tissue ischemia and home to and incorporate into sites of neovascularization (21). Similar to epithelial progenitor cells, in the present study, transplanted MSCs were preferentially attracted to and retained in the border zone of infarcts. This is consistent with recent findings in the ischemic heart (5)

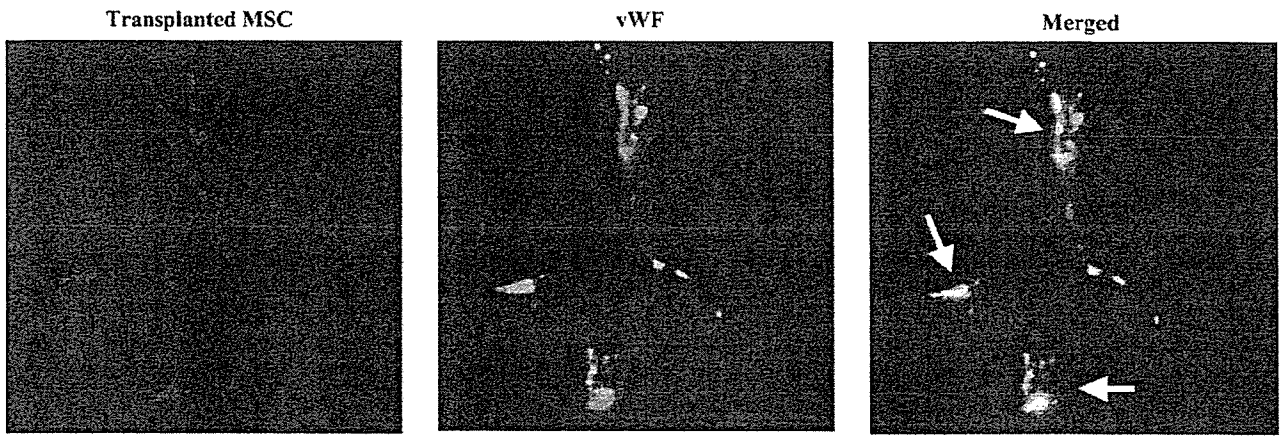

Fig. 6. Transplanted MSCs were positive for von Willebrand factor (vWF) and formed vascular structures. Magnification ×400.

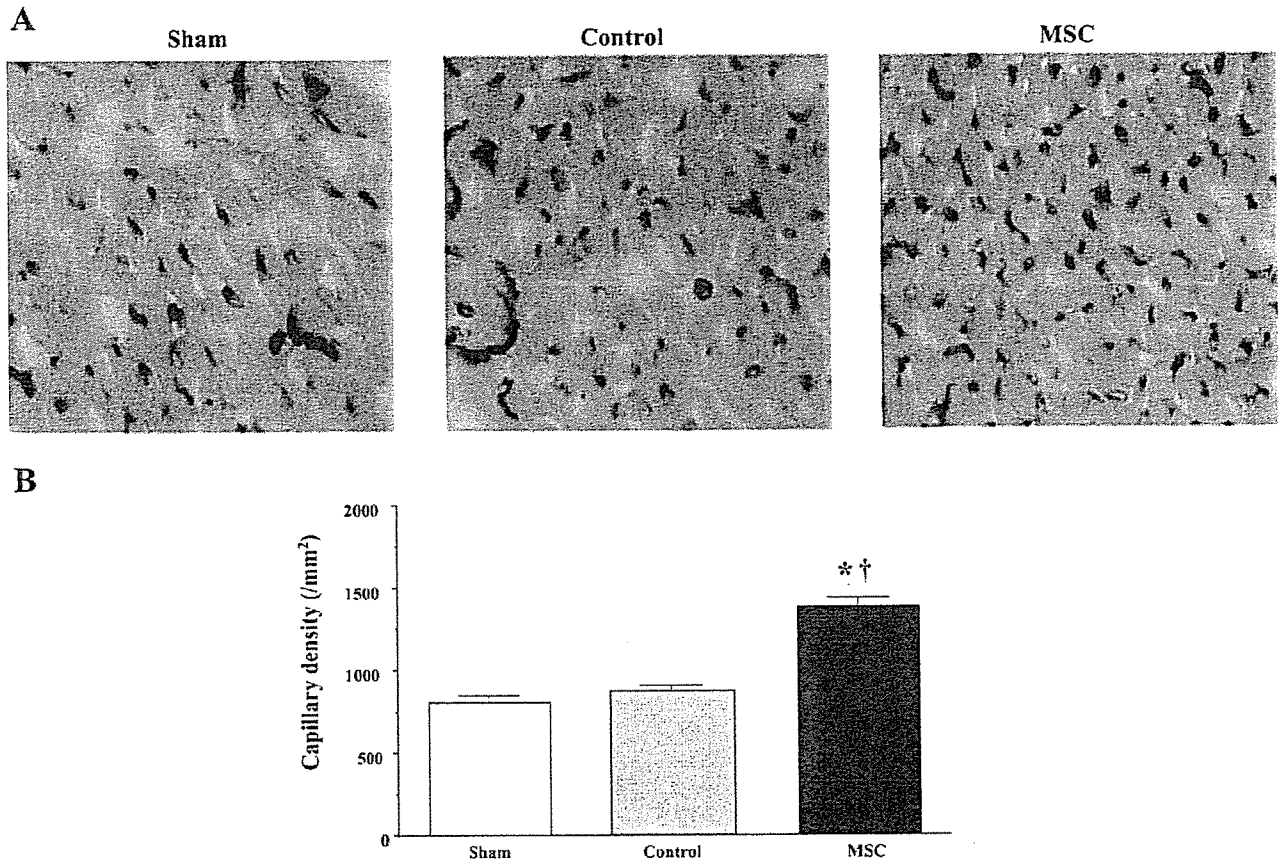

Fig. 7. *A*: representative samples of alkaline phosphatase staining in peri-infarct area. Magnification ×200. *B*: quantitative analysis of capillary density in peri-infarct area. Values are means ± SE. *$P < 0.05$ vs. sham. †$P < 0.05$ vs. control.

or brain (7). Although the underlying mechanisms remain unclear, ischemic tissue may express specific receptors or ligands to facilitate trafficking, adhesion, and infiltration of MSCs to ischemic sites.

In the present study, some of the engrafted MSCs were stained by cardiac proteins such as desmin and cardiac troponin T. Transplanted MSCs also expressed connexin43, a gap junction protein, at contact points with native cardiomyocytes. These results suggest that MSCs differentiated into cardiomyocytes in the ischemic myocardium and formed connections with native cardiomyocytes. In contrast to skeletal myoblasts, which have been used as a tool for myocardial repair, MSCs may have the capacity for electromechanical coupling. Earlier studies demonstrated the importance of the microenvironment for cardiomyogenic differentiation. Possible factors might include direct cell-cell contact (9), electrical and mechanical stimulation (10), and unknown growth factors. On the other hand, recent studies showed that stem cells may fuse with existing native cells (22, 25). Although the mechanisms by which MSCs develop into cardiomyocyte-like cells remain unclear, it is possible that the direct attachment with host cardiomyocytes in the ischemic myocardium contributes to the cardiogenic differentiation of transplanted MSCs. Further studies are necessary to investigate whether engrafted MSCs are actually becoming contractile.

In the present study, some of the transplanted MSCs were positive for an endothelial cell marker and participated in vessel formation. MSC transplantation significantly increased the capillary density in ischemic myocardium. The recently reported phenotypic plasticity of MSCs to transform into endothelial-like cells provides a rationale for their potential role in neovascularization. Hypoxia has been shown to induce MSC migration and capillary-like structure formation by upregulation of membrane type 1 matrix metalloproteinase (3). MSC implantation has been shown to induce therapeutic angiogenesis in a rat model of chronic hindlimb ischemia (1). These findings support the theory that intravenously administered MSCs are able to differentiate into vascular endothelial cells in the ischemic myocardium. Interestingly, MSCs enhance angiogenesis partly by increasing endogenous levels of vascular endothelial growth factor and vascular endothelial growth factor type 2 receptor (7). Together, these findings suggest that MSCs may contribute to neovascularization in the ischemic myocardium not only through their ability to generate capillary-like structures and but also through growth factor-mediated paracrine regulation.

The present study showed that MSC transplantation significantly reduced infarct size and attenuated wall thinning after acute myocardial infarction. Cardiomyocyte apoptosis during ischemia is one of the major contributors to the development of myocardial infarcts (16, 20). It is possible that newly formed vessels after MSC transplantation improve tissue perfusion around the ischemic boundary zone, resulting in functional recovery after acute myocardial infarction. We also demonstrated that transplanted

MSCs differentiated into cardiomyocytes in the ischemic myocardium. These results suggest that the decrease in infarct size and the increase in wall thickness may be attributable not only to MSC-induced neovascularization but also to myocardial regeneration. In the present study, MSC transplantation improved cardiac function after acute myocardial infarction, as indicated by a significant decrease in LV end-diastolic pressure, a tendency for an increase in maximum LV dP/dt, and a decrease in minimum LV dP/dt. Thus MSC-induced angiogenesis and myogenesis and the resultant reduced infarct size may have contributed to the hemodynamic improvement after acute myocardial infarction.

The low percentage of MSC migration to the heart is in agreement with some previous studies (5, 14). The present study also showed that only a small percentage of transplanted MSCs were incorporated into the heart. This may be explained by MSC apoptosis (12), tracking in the lung (5), and a dilution of the fluorescent dyes as the cells reproduce. Nevertheless, when MSCs were intravenously administered in an acute phase of myocardial infarction, MSCs induced angiogenesis and myogenesis and modestly, but significantly, improved cardiac function. Thus systemic delivery of MSCs may be beneficial for the treatment of myocardial infarction.

A limitation of this study is that the cell population may be mixed, rather than limited to MSCs, although cell surface markers of cultured cells were consistent with those of previously reported MSCs (12, 18).

In conclusion, intravenously administered MSCs were preferentially attracted to the infarcted myocardium and differentiated into vascular endothelial cells and cardiomyocytes. MSC transplantation decreased the infarct size and improved cardiac function after acute myocardial infarction through enhancement of angiogenesis and myogenesis. Thus MSC transplantation may be a new therapeutic strategy for the treatment of myocardial infarction.

GRANTS

This work was supported by Ministry of Health, Labour, and Welfare Cardiovascular Disease Research Grant 16C-6, the New Energy and Industrial Technology Development Organization of Japan Industrial Technology Research Grant Program in '03, Health and Labor Sciences Research Grants-genome 005, and Promotion of Fundamental Studies in Health Science of the Organization for Pharmaceutical Safety and Research of Japan.

REFERENCES

1. **Al-Khaldi A, Al-Sabti H, Galipeau J, and Lachapelle K.** Therapeutic angiogenesis using autologous bone marrow stromal cells: improved blood flow in a chronic limb ischemia model. *Ann Thorac Surg* 75: 204–209, 2003.
2. **Al-Khaldi A, Eliopoulos N, Martineau D, Lejeune L, Lachapelle K, and Galipeau J.** Postnatal bone marrow stromal cells elicit a potent VEGF-dependent neoangiogenic response in vivo. *Gene Ther* 10: 621–629, 2003.
3. **Annabi B, Lee YT, Turcotte S, Naud E, Desrosiers RR, Champagne M, Eliopoulos N, Galipeau J, and Beliveau R.** Hypoxia promotes murine bone-marrow-derived stromal cell migration and tube formation. *Stem Cells* 21: 337–347, 2003.
4. **Asahara T, Murohara T, Sullivan A, Silver M, van der Zee R, Li T, Witzenbichler B, Schatteman G, and Isner JM.** Isolation of putative progenitor endothelial cells for angiogenesis. *Science* 275: 964–967, 1997.
5. **Barbash IM, Chouraqui P, Baron J, Feinberg MS, Etzion S, Tessone A, Miller L, Guetta E, Zipori D, Kedes LH, Kloner RA, and Leor J.** Systemic delivery of bone marrow-derived mesenchymal stem cells to the infarcted myocardium: feasibility, cell migration, and body distribution. *Circulation* 108: 863–868, 2003.
6. **Beltrami AP, Urbanek K, Kajstura J, Yan SM, Finato N, Bussani R, Nadal-Ginard B, Silvestri F, Leri A, Beltrami CA, and Anversa P.** Evidence that human cardiac myocytes divide after myocardial infarction. *N Engl J Med* 344: 1750–1757, 2001.
7. **Chen J, Zhang ZG, Li Y, Wang L, Xu YX, Gautam SC, Lu M, Zhu Z, and Chopp M.** Intravenous administration of human bone marrow stromal cells induces angiogenesis in the ischemic boundary zone after stroke in rats. *Circ Res* 92: 692–699, 2003.
8. **Chien YW, Barbee RW, MacPhee AA, Frohlich ED, and Trippodo NC.** Increased ANF secretion after volume expansion is preserved in rats with heart failure. *Am J Physiol Regul Integr Comp Physiol* 254: R185–R191, 1988.
9. **Fukuhara S, Tomita S, Yamashiro S, Morisaki T, Yutani C, Kitamura S, and Nakatani T.** Direct cell-cell interaction of cardiomyocytes is key for bone marrow stromal cells to go into cardiac lineage in vitro. *J Thorac Cardiovasc Surg* 125: 1470–1480, 2003.
10. **Iijima Y, Nagai T, Mizukami M, Matsuura K, Ogura T, Wada H, Toko H, Akazawa H, Takano H, Nakaya H, and Komuro I.** Beating is necessary for transdifferentiation of skeletal muscle-derived cells into cardiomyocytes. *FASEB J* 17: 1361–1363, 2003.
11. **Makino S, Fukuda K, Miyoshi S, Konishi F, Kodama H, Pan J, Sano M, Takahashi T, Hori S, Abe H, Hata J, Umezawa A, and Ogawa S.** Cardiomyocytes can be generated from marrow stromal cells in vitro. *J Clin Invest* 103: 697–705, 1999.
12. **Mangi AA, Noiseux N, Kong D, He H, Rezvani M, Ingwall JS, and Dzau VJ.** Mesenchymal stem cells modified with Akt prevent remodeling and restore performance of infarcted hearts. *Nat Med* 9: 1195–1201, 2003.
13. **Messina LM, Podrazik RM, Whitehill TA, Ekhterae D, Brothers TE, Wilson JM, Burkel WE, and Stanley JC.** Adhesion and incorporation of lacZ-transduced endothelial cells into the intact capillary wall in the rat. *Proc Natl Acad Sci USA* 89: 12018–12022, 1992.
14. **Muller P, Pfeiffer P, Koglin J, Schafers HJ, Seeland U, Janzen I, Urbschat S, and Bohm M.** Cardiomyocytes of noncardiac origin in myocardial biopsies of human transplanted hearts. *Circulation* 106: 31–35, 2002.
15. **Nagaya N, Nishikimi T, Yoshihara F, Horio T, Morimoto A, and Kangawa K.** Cardiac adrenomedullin gene expression and peptide accumulation after acute myocardial infarction in rats. *Am J Physiol Regul Integr Comp Physiol* 278: R1019–R1026, 2000.
16. **Narula J, Haider N, Virmani R, DiSalvo TG, Kolodgie FD, Hajjar RJ, Schmidt U, Semigran MJ, Dec GW, and Khaw BA.** Apoptosis in myocytes in end-stage heart failure. *N Engl J Med* 335: 1182–1189, 1996.
17. **Oh H, Bradfute SB, Gallardo TD, Nakamura T, Gaussin V, Mishina Y, Pocius J, Michael LH, Behringer RR, Garry DJ, Entman ML, and Schneider MD.** Cardiac progenitor cells from adult myocardium: homing, differentiation, and fusion after infarction. *Proc Natl Acad Sci USA* 100: 12313–12318, 2003.
18. **Pittenger MF, Mackay AM, Beck SC, Jaiswal RK, Douglas R, Mosca JD, Moorman MA, Simonetti DW, Craig S, and Marshak DR.** Multilineage potential of adult human mesenchymal stem cells. *Science* 284: 143–147, 1999.
19. **Reyes M, Dudek A, Jahagirdar B, Koodie L, Marker PH, and Verfaillie CM.** Origin of endothelial progenitors in human postnatal bone marrow. *J Clin Invest* 109: 337–346, 2002.
20. **Saraste A, Pulkki K, Kallajoki M, Henriksen K, Parvinen M, and Voipio-Pulkki LM.** Apoptosis in human acute myocardial infarction. *Circulation* 95: 320–323, 1997.
21. **Shake JG, Gruber PJ, Baumgartner WA, Senechal G, Meyers J, Redmond JM, Pittenger MF, and Martin BJ.** Mesenchymal stem cell implantation in a swine myocardial infarct model: engraftment and functional effects. *Ann Thorac Surg* 73: 1919–1925, 2002.
22. **Terada N, Hamazaki T, Oka M, Hoki M, Mastalerz DM, Nakano Y, Meyer EM, Morel L, Petersen BE, and Scott EW.** Bone marrow cells adopt the phenotype of other cells by spontaneous cell fusion. *Nature* 416: 542–545, 2002.
23. **Toma C, Pittenger MF, Cahill KS, Byrne BJ, and Kessler PD.** Human mesenchymal stem cells differentiate to a cardiomyocyte phenotype in the adult murine heart. *Circulation* 105: 93–98, 2002.
24. **Wang JS, Shum-Tim D, Galipeau J, Chedrawy E, Eliopoulos N, and Chiu RC.** Marrow stromal cells for cellular cardiomyoplasty: feasibility and potential clinical advantages. *J Thorac Cardiovasc Surg* 120: 999–1005, 2000.
25. **Ying QL, Nichols J, Evans EP, and Smith AG.** Changing potency by spontaneous fusion. *Nature* 416: 545–548, 2002.

Effects of Adrenomedullin Inhalation on Hemodynamics and Exercise Capacity in Patients With Idiopathic Pulmonary Arterial Hypertension

Noritoshi Nagaya, MD; Shingo Kyotani, MD; Masaaki Uematsu, MD; Kazuyuki Ueno, PhD; Hideo Oya, MD; Norifumi Nakanishi, MD; Mikiyasu Shirai, MD; Hidezo Mori, MD; Kunio Miyatake, MD; Kenji Kangawa, PhD

Background—Adrenomedullin (AM) is a potent pulmonary vasodilator peptide. However, whether intratracheal delivery of aerosolized AM has beneficial effects in patients with idiopathic pulmonary arterial hypertension remains unknown. Accordingly, we investigated the effects of AM inhalation on pulmonary hemodynamics and exercise capacity in patients with idiopathic pulmonary arterial hypertension.

Methods and Results—Acute hemodynamic responses to inhalation of aerosolized AM (10 μg/kg body wt) were examined in 11 patients with idiopathic pulmonary arterial hypertension during cardiac catheterization. Cardiopulmonary exercise testing was performed immediately after inhalation of aerosolized AM or placebo. The work rate was increased by 15 W/min until the symptom-limited maximum, with breath-by-breath gas analysis. Inhalation of AM produced a 13% decrease in mean pulmonary arterial pressure (54±3 to 47±3 mm Hg, $P<0.05$) and a 22% decrease in pulmonary vascular resistance (12.6±1.5 to 9.8±1.3 Wood units, $P<0.05$). However, neither systemic arterial pressure nor heart rate was altered. Inhalation of AM significantly increased peak oxygen consumption during exercise (peak $\dot{V}O_2$, 14.6±0.6 to 15.7±0.6 mL · kg^{-1} · min^{-1}, $P<0.05$) and the ratio of change in oxygen uptake to that in work rate ($\Delta\dot{V}O_2/\Delta W$ ratio, 6.3±0.4 to 7.0±0.5 mL · min^{-1} · W^{-1}, $P<0.05$). These parameters remained unchanged during placebo inhalation.

Conclusions—Inhalation of AM may have beneficial effects on pulmonary hemodynamics and exercise capacity in patients with idiopathic pulmonary arterial hypertension. **(*Circulation*. 2004;109:351-356.)**

Key Words: peptides ■ hypertension, pulmonary ■ respiration ■ exercise ■ hemodynamics

Idiopathic pulmonary arterial hypertension is a rare but life-threatening disease characterized by progressive pulmonary hypertension, ultimately producing right heart failure and death.[1,2] Although a variety of vasodilators have been proposed as potential therapy for this disease over the past 30 years,[3–7] some patients ultimately require heart-lung or lung transplantation.[8,9] Thus, a novel therapeutic strategy is desirable.

Adrenomedullin (AM) is a potent, long-lasting vasodilator peptide that was originally isolated from human pheochromocytoma.[10] Immunoreactive AM has subsequently been detected in plasma and a variety of tissues, including blood vessels and lungs.[11,12] It has been reported that there are abundant binding sites for AM in the lungs.[13] We have shown that the plasma AM level increases in proportion to the severity of pulmonary hypertension and that circulating AM is partially metabolized in the lungs.[14,15] Interestingly, AM has been shown to inhibit the migration and proliferation of vascular smooth muscle cells.[16,17] These findings suggest that AM plays an important role in the regulation of pulmonary vascular tone and vascular remodeling. In fact, we have shown that short-term intravenous infusion of AM significantly decreases pulmonary vascular resistance in patients with congestive heart failure[18] or pulmonary arterial hypertension.[19] Unfortunately, however, intravenously administered AM induced systemic hypotension in such patients because of nonselective vasodilation in the pulmonary and systemic vascular beds.

More recently, inhalation of aerosolized prostacyclin and its analogue iloprost has been shown to cause pulmonary vasodilation without systemic hypotension in patients with idiopathic pulmonary arterial hypertension.[20,21] In addition, inhalant application of vasodilators does not impair gas exchange because the ventilation-matched deposition of drug

Received February 3, 2003; de novo received July 28, 2003; revision received October 15, 2003; accepted October 19, 2003

From the Department of Internal Medicine, National Cardiovascular Center, Osaka (N. Nagaya, S.K., H.O., N. Nakanishi, K.M.); the Cardiovascular Division, Kansai Rosai Hospital, Hyogo (M.U.); the Department of Pharmacy, National Cardiovascular Center, Osaka (K.U.); the Department of Cardiac Physiology, National Cardiovascular Center Research Institute, Osaka (M.S., H.M.); and the Department of Biochemistry, National Cardiovascular Center Research Institute, Osaka (K.K.), Japan

Correspondence to Noritoshi Nagaya, MD, Department of Internal Medicine, National Cardiovascular Center, 5-7-1 Fujishirodai, Suita, Osaka 565-8565, Japan. E-mail nagayann@hsp.ncvc.go.jp

Circulation is available at http://www.circulationaha.org

DOI: 10.1161/01.CIR.0000109493.05849.14

TABLE 1. Baseline Characteristics of Patients With Idiopathic Pulmonary Arterial Hypertension

Demographics	
Age, y	39±3
Male/female, n	2/9
NYHA functional class, n	
III	10
IV	1
Baseline hemodynamics	
MPAP, mm Hg	54±3
CI, L·min^{-1}·m^{-2}	2.4±0.1
PVR, Wood units	12.6±1.5
RAP, mm Hg	7±1
PCWP, mm Hg	7±1
Pulmonary function	
Sa_{O_2}, %	94±3
Sv_{O_2}, %	63±4
FVC, % predicted	86±4
FEV_1, % predicted	75±1
6-Minute walk test, m	355±35
Medication use, n	
Anticoagulant agents	10
Diuretics	9
Digitalis	7
Oral prostacyclin analogue	6
Calcium antagonists	2

NYHA indicates New York Heart Association; MPAP, mean pulmonary arterial pressure; CI, cardiac index; PVR, pulmonary vascular resistance; RAP, mean right atrial pressure; PCWP, pulmonary capillary wedge pressure; Sa_{O_2}, arterial oxygen pressure; Sv_{O_2}, mixed venous oxygen saturation; FVC, forced vital capacity; and FEV_1, forced expiratory volume in 1 second. Data are mean±SEM.

in the alveoli causes pulmonary vasodilation matched to ventilated areas.[20] In clinical settings, inhalation therapy may be more simple, noninvasive, and comfortable than continuous intravenous infusion therapy. Thus, the purpose of the present study was to investigate the effects of AM inhalation on hemodynamics and exercise capacity in patients with idiopathic pulmonary arterial hypertension.

Methods

Study Subjects

Eleven patients with idiopathic pulmonary arterial hypertension (9 women and 2 men; age, 39±3 years) were included in this study. Idiopathic pulmonary arterial hypertension was defined as pulmonary hypertension unexplained by any secondary cause, on the basis of the criteria of the National Institutes of Health registry.[1] Ten patients were classified as New York Heart Association (NYHA) functional class III and 1 as class IV (Table 1). Two of the 11 patients (18%) were acute responders who showed a significant decrease in mean pulmonary arterial pressure of ≥20% with a decrease in mean pulmonary arterial pressure to <35 mm Hg and no change or an increase in cardiac index during short-term infusion of epoprostenol. Long-term medication, including anticoagulant agents, digitalis, and diuretics, was kept constant. Vasodilator agents, such as oral prostacyclin analogue and calcium antagonists, were stopped ≥12 hours before the study procedure was begun. The ethics committee of the National Cardiovascular Center approved the study, and all patients gave written informed consent.

Preparation of Human AM

Human AM was dissolved in saline with 4% D-mannitol and sterilized by passage through a 0.22-μm filter (Millipore Co). At the time of dispensing, randomly selected vials were submitted for sterility and pyrogen testing. The chemical nature and content of the human AM in vials were verified by high-performance liquid chromatography and radioimmunoassay. All vials were stored frozen at −80°C from the time of dispensing until the time of preparation for administration.

Hemodynamic Studies

Acute hemodynamic responses to AM inhalation were assessed in all patients while they were in a stable condition during hospitalization. Hemodynamic variables, including pulmonary arterial pressure, right atrial pressure, pulmonary capillary wedge pressure, and cardiac output (in triplicate), were determined with a thermodilution catheter (TOO21H-7.5F, Baxter Co).[22] A 22-gauge cannula was inserted into a radial artery for hemodynamic measurements and blood sampling. After an equilibration period of 30 minutes, baseline hemodynamics were measured. Then, AM (10 μg/kg body wt) was inhaled as an aerosol with a jet nebulizer (Porta-Nebu, MEDIC-AID) for 15 minutes, which resulted in a cumulative dose of 400 to 600 μg AM. Hemodynamic parameters were measured at 15-minute intervals starting 15 minutes before AM inhalation until 60 minutes after inhalation. Blood samples for AM measurement were taken at 15-minute intervals from 15 minutes before inhalation until 60 minutes after the end of inhalation.

Cardiopulmonary Exercise Testing

The effects of AM inhalation on exercise capacity were examined in 10 of 11 patients; 1 patient with NYHA class IV underwent the 6-minute walk test according to decision of attending physicians. Cardiopulmonary exercise testing was performed immediately after inhalation of aerosolized AM (10 μg/kg body wt) or saline in a double-blind, randomized, crossover design. This study was performed on 2 separate days, 1 week apart. The first cardiopulmonary exercise testing was performed within 10 days after the cardiac catheterization. The patients performed exercise seated on a cycle ergometer. They first pedaled at 55 rpm without any added load for 1 minute. The work rate was then increased by 15 W/min up to the symptom-limited maximum. Breath-by-breath gas analysis was performed with an AE280 (Minato Medical Science) connected to a personal computer running analyzing software.[23] The ratio of change in oxygen uptake to that in work rate ($\Delta\dot{V}O_2/\Delta W$ ratio) was calculated as the slope of oxygen consumption per unit workload from 1 minute after the start of load addition until 85% maximal $\dot{V}O_2$. Exercise capacity was evaluated by peak oxygen consumption (peak $\dot{V}O_2$), which was defined as the value of averaged data during the final 15 seconds of exercise. Ventilatory efficiency during exercise was represented by the $\dot{V}E$-$\dot{V}CO_2$ slope, which was determined as the linear regression slope of $\dot{V}E$ and $\dot{V}CO_2$ from the start of exercise until the RC point (the time until which ventilation is stimulated by CO_2 output and end-tidal CO_2 tension begins to decrease).

Measurement of Plasma AM, cAMP, and cGMP

Blood samples were immediately transferred into chilled glass tubes containing disodium EDTA (1 mg/mL) and aprotinin (500 U/mL) and centrifuged immediately at 4°C, and the plasma was frozen and stored at −80°C until assayed. Plasma AM level was measured by a specific immunoradiometric assay kit (Shionogi Pharmaceutical Co Ltd).[24] Plasma cAMP and cGMP were determined with radioimmunoassay kits (cAMP assay kit, cGMP assay kit, Yamasa Shoyu).[18]

Statistical Analysis

All data were expressed as mean±SEM unless otherwise indicated. Changes in hemodynamic and hormonal parameters by AM inhalation were analyzed by 1-way ANOVA for repeated measures,

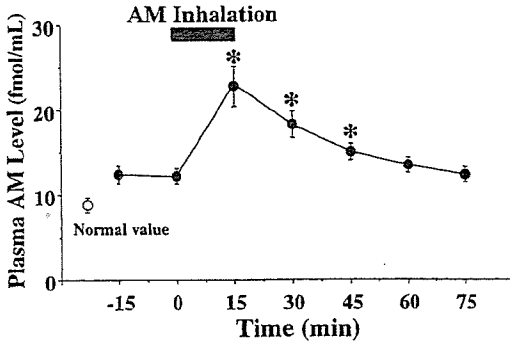

Figure 1. Changes in plasma AM level by inhalation of aerosolized AM in patients with idiopathic pulmonary arterial hypertension. Normal value indicates plasma AM level derived from 15 age-matched healthy subjects. Data are mean±SEM. *$P<0.05$ vs value at time 0.

followed by Newman-Keuls test. Comparisons of exercise parameters between the 2 groups were analyzed with paired Student's t test. A probability value of $P<0.05$ was considered statistically significant.

Results

All patients tolerated this study protocol. One patient developed a headache, and another patient had mild arterial hypoxemia during AM inhalation. None of them experienced other adverse effects, such as systemic hypotension, infection, or arrhythmia.

Plasma AM Level After Inhalation

Baseline plasma AM level in patients with idiopathic pulmonary arterial hypertension was significantly higher than the normal value, which was determined from pooled data of 15 age-matched healthy subjects (11.9±0.8 versus 9.3±0.1 fmol/mL, $P<0.05$). Inhalation of AM significantly increased the plasma AM level to 22.9±2.1 fmol/mL immediately after inhalation (Figure 1). The half-life of plasma AM after inhalation was approximately 20 minutes, and the elevation of AM lasted for >45 minutes. Plasma cAMP level increased significantly 30 minutes after the initiation of AM inhalation (10.8±0.7 to 12.0±0.6 pmol/mL, $P<0.05$), although plasma cGMP level was not significantly altered (6.5±1.0 to 6.8±1.0 pmol/mL, P=NS).

Hemodynamic Effects of AM Inhalation

Inhalation of AM significantly decreased mean pulmonary arterial pressure in patients with idiopathic pulmonary arterial hypertension (54±3 to 47±3 mm Hg, $P<0.05$) without a significant decrease in mean arterial pressure (85±4 to 83±4 mm Hg, P=NS) (Figure 2). AM inhalation slightly but significantly increased cardiac index by 12% (2.4±0.1 to 2.7±0.2 L · min^{-1} · m^{-2}, $P<0.05$). Thus, AM inhalation resulted in a 22% decrease in pulmonary vascular resistance (12.6±1.5 to 9.8±1.3 Wood units, $P<0.05$) (Figure 3). Inhaled AM did not significantly alter systemic vascular resistance. The ratio of pulmonary vascular resistance to systemic vascular resistance was decreased significantly at the end of inhalation (0.63±0.08 to 0.55±0.07, $P<0.05$). These hemodynamic effects of AM lasted for >45 minutes.

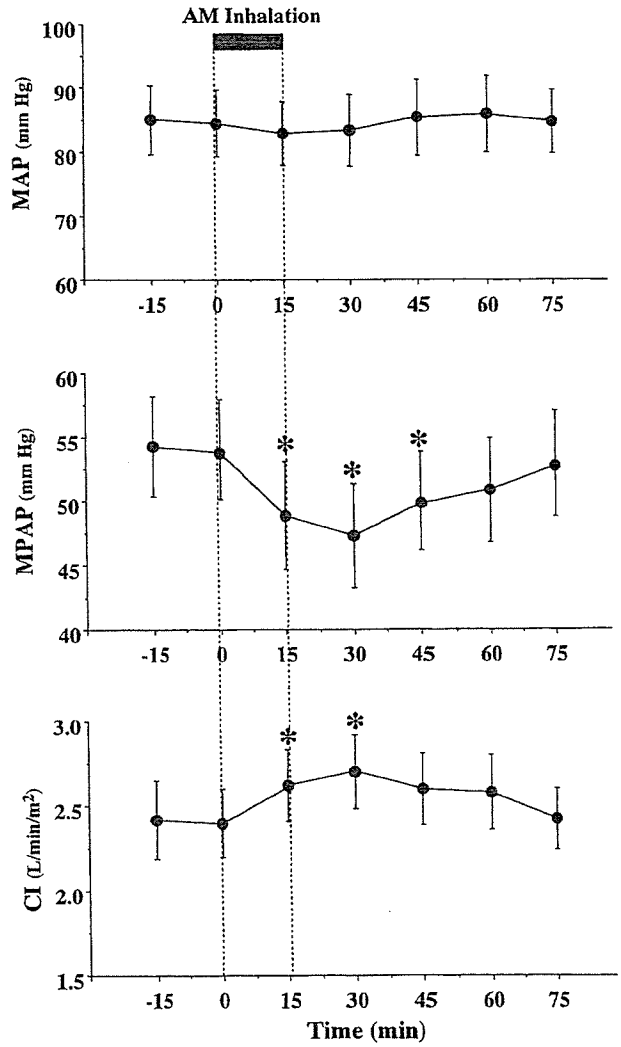

Figure 2. Changes in mean arterial pressure (MAP), mean pulmonary arterial pressure (MPAP), and cardiac index (CI) by inhalation of aerosolized AM in patients with idiopathic pulmonary arterial hypertension. Data are mean±SEM. *$P<0.05$ vs value at time 0.

No significant change in heart rate, pulmonary capillary wedge pressure, or right atrial pressure was observed. There was no significant change in arterial oxygen saturation (94±3% to 93±3%).

Effects of AM Inhalation on Exercise Capacity and Ventilatory Efficiency

As the limiting symptom at the end of exercise, 6 patients reported muscle weakness and 4 reported dyspnea. There was no difference in these symptoms when exercise testing was performed with or without inhalation of AM. Inhalation of AM altered neither heart rate nor blood pressure either at rest or at peak exercise (Table 2). Inhalation of AM significantly increased peak workload (86±5 to 93±6 W, $P<0.05$) (Table 2). AM also significantly increased peak $\dot{V}O_2$ (14.6±0.6 to 15.7±0.6 mL · kg^{-1} · min^{-1}, $P<0.05$) (Figure 4). Inhalation of AM significantly increased $\Delta\dot{V}O_2/\Delta W$ ratio (6.3±0.4 to

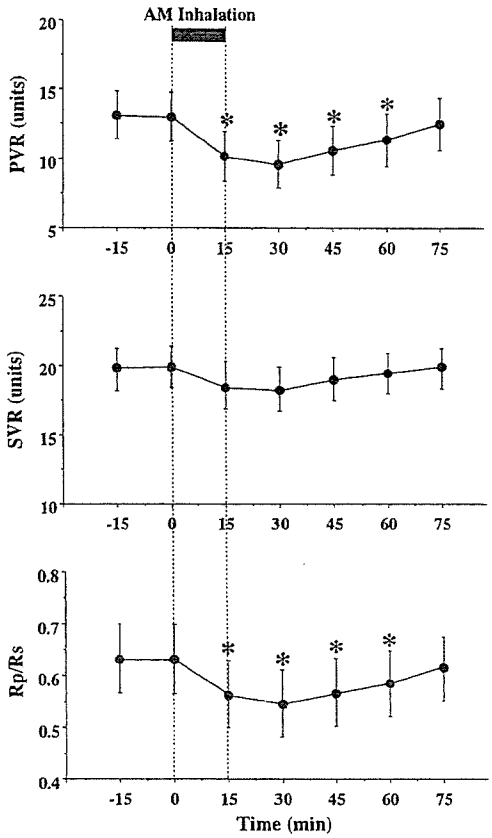

Figure 3. Changes in pulmonary vascular resistance (PVR), systemic vascular resistance (SVR), and ratio of pulmonary vascular resistance to systemic vascular resistance (Rp/Rs) by inhalation of aerosolized AM in patients with idiopathic pulmonary arterial hypertension. Data are mean ± SEM. *$P<0.05$ vs value at time 0.

7.0±0.5 mL · min^{-1} · W^{-1}, $P<0.05$). AM did not significantly alter the $\dot{V}_E$-$\dot{V}_{CO_2}$ slope (Table 2). No significant changes in arterial oxygen saturation were observed either at rest or at peak exercise. In 1 patient with NYHA class IV who did not undergo cardiopulmonary exercise testing, the distance walked in 6 minutes increased from 150 to 180 m by inhalation of AM.

Discussion

In the present study, we demonstrated that inhalation of AM improved hemodynamics with pulmonary selectivity and exercise capacity in patients with idiopathic pulmonary arterial hypertension.

AM is one of the most potent endogenous vasodilators in the pulmonary vascular bed.[25–27] The vasodilatory effect is mediated by cAMP-dependent and nitric oxide–dependent mechanisms.[28,29] Endogenous AM production is enhanced in a variety of cardiovascular diseases through a compensatory mechanism.[14,30] Nonetheless, additional supplementation of AM has beneficial effects in these diseases.[18,19] These results suggest that endogenous AM level is not sufficient to improve deteriorated conditions despite the increased AM production. Interestingly, Champion et al[31] have shown that intratracheal gene transfer of calcitonin gene–related peptide, a member of the same peptide family as AM, to bronchial

TABLE 2. Changes in Exercise Parameters by Inhalation of AM or Placebo

Variables	Placebo	AM	P
Peak workload, W	86±5	93±6	<0.05
HR, bpm			
Rest	75±5	75±3	NS
Peak	144±6	148±6	NS
MAP, mm Hg			
Rest	85±3	87±5	NS
Peak	108±5	110±6	NS
Peak Borg score (D/L)	17/18	18/18	NS
Peak $\dot{V}o_2$, mL · kg^{-1} · min^{-1}	14.6±0.6	15.7±0.6	<0.05
$\Delta\dot{V}o_2/\Delta W$ ratio, mL · min^{-1} · W^{-1}	6.3±0.4	7.0±0.5	<0.05
$\dot{V}_E$-$\dot{V}co_2$ slope	37±2	36±2	NS
Sao_2, %			
Rest	97±1	97±1	NS
Peak	95±1	95±1	NS

HR indicates heart rate; MAP, mean arterial pressure; Peak Borg score (D/L), Borg score at peak exercise (dyspnea/leg fatigue); Peak $\dot{V}o_2$, peak oxygen consumption; $\Delta\dot{V}o_2/\Delta W$ ratio, $\dot{V}o_2$ increase per unit workload; $\dot{V}_E$-$\dot{V}co_2$ slope, slope of regression line of relation between $\dot{V}_E$ and $\dot{V}co_2$; and Sao_2, arterial oxygen saturation. Data are mean ± SEM.

epithelial cells attenuates chronic hypoxia-induced pulmonary hypertension in the mouse. These results raise the possibility that intratracheal delivery of a vasodilator peptide may be sufficient to alter pulmonary vascular function. In fact, in the present study, inhalation of AM significantly decreased pulmonary vascular resistance, whereas it did not alter systemic arterial pressure or systemic vascular resistance. The ratio of pulmonary vascular resistance to systemic vascular resistance was reduced significantly by AM inhalation. These results suggest that inhaled AM improves hemodynamics with pulmonary selectivity. This is consistent with earlier findings that inhaled prostacyclin or its analogue iloprost acts transepithelially with pulmonary selectivity and improves pulmonary hypertension.[20,21] Inhalation of AM slightly but significantly increased cardiac index in patients with idiopathic pulmonary arterial hypertension. Considering the strong vasodilator activity of AM in the pulmonary vasculature, the significant decrease in cardiac afterload may be responsible for increased cardiac index with

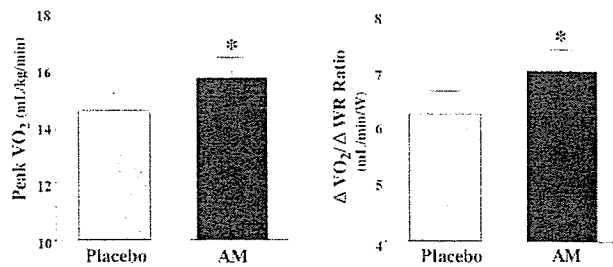

Figure 4. Changes in peak oxygen consumption (peak $\dot{V}o_2$) and ratio of change in oxygen uptake to that in work rate ($\Delta\dot{V}o_2/\Delta W$ ratio) by inhalation of aerosolized AM or placebo in patients with idiopathic pulmonary arterial hypertension. Data are mean ± SEM. *$P<0.05$ vs placebo.

AM. Interestingly, the hemodynamic effects of inhaled AM lasted for >45 minutes. A previous study demonstrated that intravenous injection of AM produces a long-lasting vasodilator response because of its long half-life (≈15 minutes).[32] The half-life of plasma AM after inhalation was longer (20 minutes). Thus, inhalation of AM may cause relatively long-lasting pulmonary vasodilator activity in patients with idiopathic pulmonary arterial hypertension. In the present study, plasma cAMP level increased after AM inhalation, suggesting that the hemodynamic effects of AM may be mediated by activation of cAMP.

Earlier studies have shown that peak $\dot{V}o_2$ during exercise is markedly lower in patients with idiopathic pulmonary arterial hypertension than in healthy subjects.[33,34] Peak $\dot{V}o_2$ is determined primarily by the maximal cardiac output during exercise and the potential for O_2 extraction by the exercising muscle.[35] Thus, the decreased peak $\dot{V}o_2$ may reflect insufficient oxygen delivery to the body during exercise, at least in part because of an inadequate increase in cardiac output under conditions of severe pulmonary hypertension. In the present study, inhalation of AM significantly increased peak $\dot{V}o_2$ in patients with pulmonary hypertension. AM also increased the $\Delta\dot{V}o_2/\Delta W$ ratio, which indicates oxygen transport per unit workload to the exercising legs. These results suggest that inhalation of AM improves exercise capacity in patients with idiopathic pulmonary arterial hypertension. It is possible that an increase in cardiac output during exercise may contribute to increases in peak $\dot{V}o_2$ and the $\Delta\dot{V}o_2/\Delta W$ ratio.

The major limitation of this pilot trial relates to the lack of a randomized, placebo-controlled group in acute hemodynamic studies, which was as result not only of invasive assessment of hemodynamics but also of the limited number of patients available. Nevertheless, cardiopulmonary exercise testing was performed in a double-blind, randomized, crossover design. Thus, it is unlikely that the hemodynamic effects of inhaled AM are attributable to the placebo effect.

Inhalation therapy may be more simple, noninvasive, and comfortable than continuous intravenous infusion therapy. An experimental study demonstrated that repeated inhalation of AM (for 30 minutes, 4 times a day) inhibited monocrotaline-induced pulmonary hypertension and markedly improved survival in rats.[36] Recently, pulmonary delivery of a dry-powder insulin has been shown to improve glycemic control without adverse pulmonary effects.[37] Although further studies are necessary to maximize the efficiency and reproducibility of pulmonary AM delivery, combining AM inhalation therapy with other modalities that have a different mode of action may have beneficial effects in patients with idiopathic pulmonary arterial hypertension.

Conclusions

These preliminary results suggest that inhalation of AM may have beneficial effects on pulmonary hemodynamics and exercise capacity in patients with idiopathic pulmonary arterial hypertension.

Acknowledgments

This work was supported by grants from NEDO, the Mochida Memorial Foundation for Medical and Pharmaceutical Research, the Japan Cardiovascular Research Foundation, Health and Labor Sciences Research grant genome 005, and the Promotion of Fundamental Studies in Health Science of the Organization for Pharmaceutical Safety and Research of Japan. We thank Masahiko Shibakawa for preparing AM.

References

1. Rich S, Dantzker DR, Ayres SM, et al. Primary pulmonary hypertension: a national prospective study. *Ann Intern Med*. 1987;107:216–223.
2. Rich S. Primary pulmonary hypertension. *Prog Cardiovasc Dis*. 1988;31:205–238.
3. Rubin LJ, Peter RH. Oral hydralazine therapy for primary pulmonary hypertension. *N Engl J Med*. 1980;302:69–73.
4. Rich S, Kaufmann E, Levy PS. The effect of high doses of calcium-channel blockers on survival in primary pulmonary hypertension. *N Engl J Med*. 1992;327:76–81.
5. Barst RJ, Rubin LJ, Long WA, et al. A comparison of continuous intravenous epoprostenol (prostacyclin) with conventional therapy for primary pulmonary hypertension. *N Engl J Med*. 1996;334:296–301.
6. McLaughlin VV, Genthner DE, Panella MM, et al. Reduction in pulmonary vascular resistance with long-term epoprostenol (prostacyclin) therapy in primary pulmonary hypertension. *N Engl J Med*. 1998;338:273–277.
7. Nagaya N, Uematsu M, Okano Y, et al. Effect of orally active prostacyclin analogue on survival of outpatients with primary pulmonary hypertension. *J Am Coll Cardiol*. 1999;34:1188–1192.
8. Reitz BA, Wallwork JL, Hunt SA, et al. Heart-lung transplantation: successful therapy for patients with pulmonary vascular disease. *N Engl J Med*. 1982;306:557–564.
9. Pasque MK, Trulock EP, Kaiser LD, et al. Single lung transplantation for pulmonary hypertension: three month hemodynamic follow-up. *Circulation*. 1991;84:2275–2279.
10. Kitamura K, Kangawa K, Kawamoto M, et al. Adrenomedullin: a novel hypotensive peptide isolated from human pheochromocytoma. *Biochem Biophys Res Commun*. 1993;192:553–560.
11. Ichiki Y, Kitamura K, Kangawa K, et al. Distribution and characterization of immunoreactive adrenomedullin in human tissue and plasma. *FEBS Lett*. 1994;338:6–10.
12. Sakata J, Shimokubo T, Kitamura K, et al. Distribution and characterization of immunoreactive rat adrenomedullin in tissue and plasma. *FEBS Lett*. 1994;352:105–108.
13. Owji AA, Smith DM, Coppock HA, et al. An abundant and specific binding site for the novel vasodilator adrenomedullin in the rat. *Endocrinology*. 1995;136:2127–2134.
14. Kakishita M, Nishikimi T, Okano Y, et al. Increased plasma levels of adrenomedullin in patients with pulmonary hypertension. *Clin Sci*. 1999;96:33–39.
15. Yoshibayashi M, Kamiya T, Kitamura K, et al. Plasma levels of adrenomedullin in primary and secondary pulmonary hypertension in patients ≤ 20 years of age. *Am J Cardiol*. 1997;79:1556–1558.
16. Horio T, Kohno M, Kano H, et al. Adrenomedullin as a novel antimigration factor of vascular smooth muscle cells. *Circ Res*. 1995;77:660–664.
17. Kano H, Kohno M, Yasunari K, et al. Adrenomedullin as a novel antiproliferative factor of vascular smooth muscle cells. *J Hypertens*. 1996;14:209–213.
18. Nagaya N, Satoh T, Nishikimi T, et al. Hemodynamic, renal, and hormonal effects of adrenomedullin infusion in patients with congestive heart failure. *Circulation*. 2000;101:498–503.
19. Nagaya N, Nishikimi T, Uematsu M, et al. Haemodynamic and hormonal effects of adrenomedullin in patients with pulmonary hypertension. *Heart*. 2000;84:653–658.
20. Walmrath D, Schneider T, Pilch J, et al. Aerosolized prostacyclin reduces pulmonary artery pressure and improves gas exchange in the adult respiratory distress syndrome (ARDS). *Lancet*. 1993;342:961–962.
21. Hoeper MM, Schwarze M, Ehlerding S, et al. Long-term treatment of primary pulmonary hypertension with aerosolized iloprost, a prostacyclin analogue. *N Engl J Med*. 2000;342:1866–1870.
22. Rich S, Seidlitz M, Dodin E, et al. The short-term effects of digoxin in patients with right ventricular dysfunction from pulmonary hypertension. *Chest*. 1998;114:787–792.
23. Miyamoto S, Nagaya N, Satoh T, et al. Clinical correlates and prognostic significance of six-minute walk test in patients with primary pulmonary

hypertension: comparison with cardiopulmonary exercise testing. *Am J Respir Crit Care Med*. 2000;161:487–492.
24. Ohta H, Tsuji T, Asai S, et al. A simple immunoradiometric assay for measuring the entire molecules of adrenomedullin in human plasma. *Clin Chim Acta*. 1999;287:131–143.
25. Lippton H, Chang JK, Hao Q, et al. Adrenomedullin dilates the pulmonary vascular bed in vivo. *J Appl Physiol*. 1994;76:2154–2156.
26. Heaton J, Lin B, Chang JK, et al. Pulmonary vasodilation to adrenomedullin: a novel peptide in humans. *Am J Physiol*. 1995;268:H2211–H2215.
27. Nossaman BD, Feng CJ, Kaye AD, et al. Pulmonary vasodilator responses to adrenomedullin are reduced by NOS inhibitors in rats but not in cats. *Am J Physiol*. 1996;270:L782–L789.
28. Ishizaka Y, Ishizaka Y, Tanaka M, et al. Adrenomedullin stimulates cyclic AMP formation in rat vascular smooth muscle cells. *Biochem Biophys Res Commun*. 1994;200:642–646.
29. Nakamura M, Yoshida H, Makita S, et al. Potent and long-lasting vasodilatory effects of adrenomedullin in humans: comparisons between normal subjects and patients with chronic heart failure. *Circulation*. 1997;95:1214–1221.
30. Nagaya N, Nishikimi T, Yoshihara F, et al. Cardiac adrenomedullin gene expression and peptide accumulation after acute myocardial infarction in rats. *Am J Physiol*. 2000;278:R1019–R1026.
31. Champion HC, Bivalacqua TJ, Toyoda K, et al. In vivo gene transfer of prepro-calcitonin gene-related peptide to the lung attenuates chronic hypoxia-induced pulmonary hypertension in the mouse. *Circulation*. 2000;101:931–937.
32. Ishiyama Y, Kitamura K, Ichiki Y, et al. Haemodynamic responses to rat adrenomedullin in anaesthetized spontaneously hypertensive rats. *Clin Exp Pharmacol Physiol*. 1995;22:614–618.
33. D'Alonzo GE, Gianotti LA, Pohil RL, et al. Comparison of progressive exercise performance of normal subjects and patients with primary pulmonary hypertension. *Chest*. 1987;92:57–62.
34. Wensel R, Opitz CF, Anker SD, et al. Assessment of survival in patients with primary pulmonary hypertension: importance of cardiopulmonary exercise testing. *Circulation*. 2002;106:319–324.
35. Anderson P, Saltin B. Maximal perfusion of skeletal muscle in man. *J Appl Physiol*. 1985;366:233–249.
36. Nagaya N, Okumura H, Uematsu M, et al. Repeated inhalation of adrenomedullin ameliorates pulmonary hypertension and survival in monocrotaline rats. *Am J Physiol Heart Circ Physiol*. 2003;285:H2125–H2131.
37. Skyler JS, Cefalu WT, Kourides IA, et al. Efficacy of inhaled human insulin in type 1 diabetes mellitus: a randomised proof-of-concept study. *Lancet*. 2001;357:331–335.

0026-895X/04/6603-667–674$20.00
MOLECULAR PHARMACOLOGY
Copyright © 2004 The American Society for Pharmacology and Experimental Therapeutics
Mol Pharmacol 66:667–674, 2004

Vol. 66, No. 3
2626/1172525
Printed in U.S.A.

γ-Mangostin Inhibits Inhibitor-κB Kinase Activity and Decreases Lipopolysaccharide-Induced Cyclooxygenase-2 Gene Expression in C6 Rat Glioma Cells

Keigo Nakatani,[1] Tohru Yamakuni, Nobuhiko Kondo, Tsutomu Arakawa, Kenji Oosawa, Susumu Shimura, Hiroyasu Inoue, and Yasushi Ohizumi

Department of Pharmaceutical Molecular Biology, Graduate School of Pharmaceutical Sciences, Tohoku University, Sendai, Japan (K.N., T.Y., N.K., Y.O.); Central Laboratory, Lotte Co., Ltd., Saitama, Japan (T.A., K.O., S.S.); and Department of Pharmacology, National Cardiovascular Center Research Institute, Osaka, Japan (H.I.)

Received May 11, 2004; accepted June 18, 2004

ABSTRACT

We investigated the effect of γ-mangostin purified from the fruit hull of the medicinal plant *Garcinia mangostana* on spontaneous prostaglandin E_2 (PGE_2) release and inducible cyclooxygenase 2 (COX-2) gene expression in C6 rat glioma cells. An 18-h treatment with γ-mangostin potently inhibited spontaneous PGE_2 release in a concentration-dependent manner with the IC_{50} value of approximately 2 μM, without affecting the cell viability even at 30 μM. By immunoblotting and reverse-transcription polymerase chain reaction, we showed that γ-mangostin concentration-dependently inhibited lipopolysaccharide (LPS)-induced expression of COX-2 protein and its mRNA, but not those of constitutive COX-1 cyclooxygenase. Because LPS is known to stimulate inhibitor κB (IκB) kinase (IKK)-mediated phosphorylation of IκB followed by its degradation, which in turn induces nuclear factor (NF)-κB nuclear translocation leading to transcriptional activation of COX-2 gene, the effect of γ-mangostin on the IKK/IκB cascade controlling the NF-κB activation was examined. An in vitro IKK assay using IKK protein immunoprecipitated from C6 cell extract showed that this compound inhibited IKK activity in a concentration-dependent manner, with the IC_{50} value of approximately 10 μM. Consistently γ-mangostin was also observed to decrease the LPS-induced IκB degradation and phosphorylation in a concentration-dependent manner, as assayed by immunoblotting. Furthermore, luciferase reporter assays showed that γ-mangostin reduced the LPS-inducible activation of NF-κB–and human COX-2 gene promoter region-dependent transcription. γ-Mangostin also inhibited rat carrageenan-induced paw edema. These results suggest that γ-mangostin directly inhibits IKK activity and thereby prevents COX-2 gene transcription, an NF-κB target gene, probably to decrease the inflammatory agent-stimulated PGE_2 production in vivo, and is a new useful lead compound for anti-inflammatory drug development.

Prostaglandins (PGs), arachidonic acid (AA) metabolites of the cyclooxygenase (COX) pathway, are major mediators in the regulation of inflammation and immune function (Smith et al., 2000). In the brain, the prostaglandin E_2 (PGE_2) is the most abundant PG. PGE_2 levels are very low or undetectable in normal conditions but can rise in response to inflammatory processes, multiple sclerosis, and AIDS-associated dementia (Fretland, 1992; Griffin et al., 1994). High levels of PGE_2 can modulate the activities of multiple cell types, including neurons, glial, and endothelial cells, as well as microglia/macrophage and lymphocyte functions during inflammatory and immune processes (Weissmann, 1993). Astrocytes are a known important source of PGE_2 in the CNS (Katsuura et al., 1989). Their ability to produce PGE_2 upon stimulation with interleukin (IL)-1β, tumor necrosis factor-α (TNF-α), or bacterial wall protein lipopolysaccharide (LPS) has been extensively documented (Fontana et al., 1982; Mollace et al., 1998; Molina-Holgado et al., 2000).

Cyclooxygenase (COX) is well known to be responsible for PG production and the rate-limiting enzymes. This enzyme

This work was partly supported by a Grant-in-Aid for Scientific Research from the Ministry of Education, Science, Sport and Culture of Japan.

[1] Current address: Pfizer Global Research and Development, Nagoya Laboratories, Aichi, Japan.

Article, publication date, and citation information can be found at http://molpharm.aspetjournals.org.
doi:10.1124/mol.104.002626.

ABBREVIATIONS: PG, prostaglandin; AA, arachidonic acid; COX, cyclooxygenase; COX-1, constitutive cyclooxygenase; COX-2, inducible cyclooxygenase; PGE_2, prostaglandin E_2; LPS, lipopolysaccharide; IκB, inhibitor κB; IKK, inhibitor κB kinase; CNS, central nervous system; IL, interleukin; TNF-α, tumor necrosis factor-α; NF-κB, nuclear factor-κB; MTT, 3-(4,5-dimethylthiazol-2-yl)-2,5-diphenyltetrazolium; RT, reverse transcription; PCR, polymerase chain reaction; PAGE, polyacrylamide gel electrophoresis; ODS, octadecylsilyl; HPLC, high-performance liquid chromatography; DMSO, dimethyl sulfoxide; NS398, *N*-[2-(cyclohexyloxyl)-4-nitrophenyl]-methane sulfonamide.

exists as two isoforms, namely constitutive COX (COX-1) and inducible COX (COX-2). COX-2 gene is an early-inducible gene in response to many inflammatory cytokines, including IL-1, TNF-α, and LPS. COX-2 gene expression is controlled at the transcriptional and/or the post-transcriptional levels (Dixon et al., 2000). The promoter regions of COX-2 gene of rat, human, and mouse have been extensively analyzed (Sirois et al., 1993; Appleby et al., 1994; Kosaka et al., 1994; Inoue et al., 1995) and have been shown to contain potential binding sites for various transcriptional factors, some of which have been demonstrated to be indeed functional (Goppelt-Struebe, 1995). For example, activation of nuclear factor-κB (NF-κB) has been reported recently to actually participate in the transcriptional activation of COX-2 gene induced by IL-1 (Newton et al., 1997), TNF-α (Yamamoto et al., 1995), and LPS (Inoue and Tanabe, 1998). Furthermore, the LPS-induced activation of COX-2 gene evidently has been shown to be mediated by inhibitor κB (IκB) kinase (IKK), which specifically catalyzes IκB phosphorylation followed by its degradation and the subsequent NF-κB nuclear translocation, leading to a stimulation of the *cis*-acting κB element-mediated transcription (Griseavage et al., 1996).

Because the fruit hull of mangosteen, *Garcinia mangostana*, has been used for many years as traditional medicine for the treatment of skin infection, wounds, and diarrhea in Southeast Asia—that is, the fruit hull exhibits an anti-inflammatory action—we pharmacologically studied the anti-inflammatory components of the fruit hull of mangosteen. In an earlier study, we examined the effect of γ-mangostin, a tetraoxygenated diprenylated xanthone from the fruit hull of this plant (Fig. 1A), on AA cascade in C6 rat glioma cells, which is well known to be a useful model system for the study of PG production in the astrocytes, and demonstrated that this natural product reduces PGE_2 release from C6 glioma cells with an IC_{50} of approximately 5 μM and potently inhibits the activities of both COX-1 and COX-2 enzymes with the IC_{50} values of approximately 0.8 and 2 μM, respectively, in vitro (Nakatani et al., 2002).

Herein, we describe the first evidence that γ-mangostin directly inhibits IKK activity, which specifically phosphorylates IκB, and thereby prevents its degradation and, as a result, induces a decrease in the expression of COX-2 protein and its mRNA by a suppression of NF-κB–dependent transcription. This study also demonstrated that γ-mangostin inhibited rat carrageenan-induced hind paw edema, an in vivo acute model of inflammation.

Materials and Methods

Materials. PGE_2 was a generous gift from Ono Pharmaceuticals (Osaka, Japan). Fetal bovine serum, horse serum, Ham's F-10 medium, Eagle's minimum essential medium, 3-(4,5-dimethylthiazol-2-yl)-2,5-diphenyltetrazolium bromide (MTT), and NS398, a selective inhibitor of COX-2, were purchased from Cell Culture Laboratory (Cleveland, OH), Dainippon Pharmaceutical Co. Ltd. (Osaka, Japan), Invitrogen (Carlsbad, CA), Nissui (Tokyo, Japan), Dojindo (Kumamoto, Japan), and Calbiochem (San Diego, CA), respectively. Anti-COX-1, anti-COX-2, anti-IκB, anti-phospho-IκB, anti-IKKα/β, and anti-actin antibodies and recombinant IκBα fusion protein (1–317), anti-PGE_2 antibody, and protein A Sepharose 4B were obtained from Santa Cruz Biochemicals (Santa Cruz, CA), Chemicon International (Temecula, CA), and Zymed Laboratories (South San Francisco, CA), respectively. Alkaline phosphatase-conjugated affinity-purified anti-goat IgG and horseradish peroxide-conjugated affinity-purified anti-rabbit IgG were from Rockland (Gilbertsville, PA) and Cell Signaling Technology Inc. (Beverly, MA), respectively. Total RNA extraction and reverse-transcription polymerase chain reaction (RT-PCR) kits, EndoFree Plasmid Maxi Kit, and pRG-TK vector and Dual-Luciferase Reporter Assay System were purchased from Toyobo Engineering (Osaka, Japan), QIAGEN K.K. (Tokyo, Japan), and Promega (Madison, WI), respectively. [^{3}H]PGE_2 (200 Ci/mmol) and [γ-^{32}P]ATP (5000 Ci/mmol) were from PerkinElmer Life and Analytical Sciences (Boston, MA) and Amersham Biosciences Inc. (Piscataway, NJ), respectively. Other chemicals and drugs were of reagent grade or of the highest quality.

Extraction and Isolation of γ-Mangostin. γ-Mangostin (Fig. 1A) was obtained from the fruit hull of *G. mangostana* L. as reported previously (Jefferson et al., 1970). In brief, the dried fruit hull (1 kg) was ground and then extracted with ethanol (10 liters) for 1 h. The ethanol extract was partitioned between ethyl acetate and water to afford an ethyl acetate fraction (87.4 g). The ethyl acetate soluble fraction was dissolved in hexane/ethyl acetate (4:1) and subjected on a silica gel column chromatography (Wakogel C-200, 800 g, a diameter of 11 cm; Wako Pure Chemicals, Tokyo, Japan), and the sample was eluted with a step-wise gradient of hexane/ethyl acetate [3:1 (2 liters), 3:2 (1 liter), 1:1 (1 liter), 2:3 (1 liter), and 3:7 (2 liters)]. After collecting 1400 ml of the first eluent, the subsequent eluent was

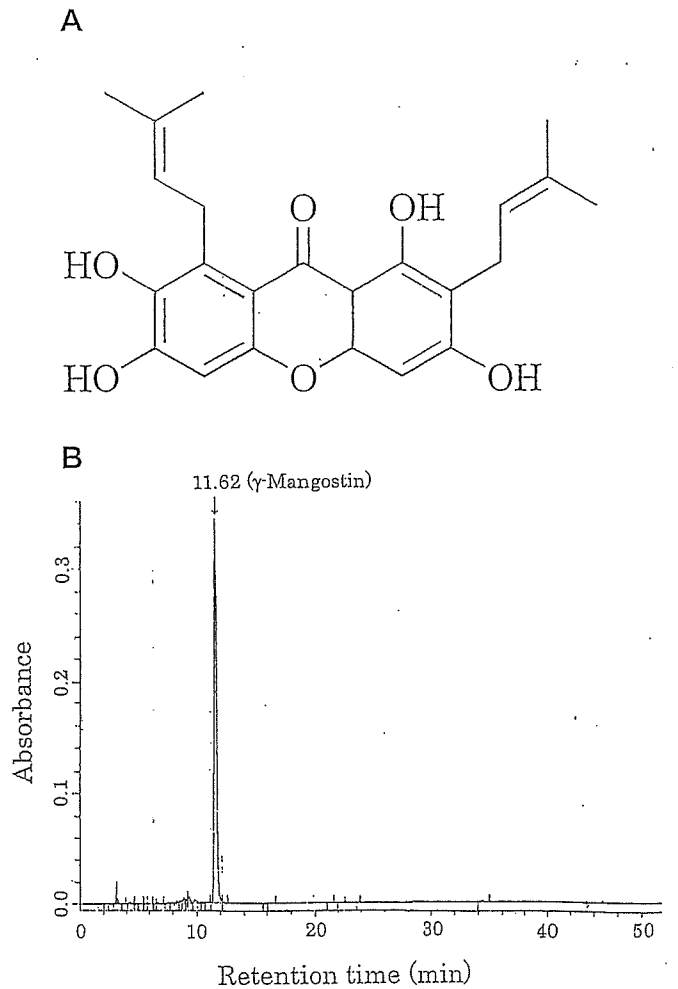

Fig. 1. Chemical structure of γ-mangostin (A) and analysis of purified γ-mangostin by HPLC (B). The elution profile was obtained by monitoring at UV absorbance of 280 nm using an HPLC column (SenshuPak ODS-1251-SS, 4.5 × 250 mm; elution: a linear gradient of 65 to 100% CH_3CN in H_2O at 1 ml/min before which the column was washed with 65% CH_3CN in H_2O for 60 min).

fractionated (200 ml each). Each fraction was monitored by thin layer chromatography [ODS silica gel; acetonitrile/water (8:2) as the developing solvent], and thereby the γ-mangostin-rich fractions, which contained γ-mangostin (R_f = 0.49) but not α-mangostin (R_f = 0.38), were combined. This silica gel column chromatography was performed two times additionally to further obtain the γ-mangostin fraction. The combined γ-mangostin fractions (17.8 g) underwent chromatography on a Senshupak PEGSIL ODS column (20 × 250 mm; Senshu Scientific Co., Tokyo, Japan) and were eluted with methanol/water (4:1 to 1:0) to yield partially purified γ-mangostin (9.0 g). The partially purified γ-mangostin fraction was subjected to an Ultra Pack Silica gel column chromatography (50 mm x 300 mm) (Yamazen, Schaumburg, IL) and eluted with hexane/ethyl acetate (1:1) followed by recrystalization in hexane to finally give purified γ-mangostin (6.0 g). Its purity was more than 90%, as determined by HPLC (SenshuPak ODS-1251-SS, 4.5 × 250 mm; Senshu Scientific) (Fig. 1B). As shown in Fig. 1B, each of the other constituents was less than 3%. Purified γ-mangostin was dissolved in dimethyl sulfoxide (DMSO) to make a concentration of 20 mM as a stock solution and diluted to appropriate concentrations before use.

Cell Culture. C6 rat glioma cells were grown in Ham's F-10 medium containing 15% horse serum and 2.5% fetal bovine serum in a 37°C humidified incubator in an atmosphere of 5% CO_2 in air (Nakatani et al., 2002).

PGE_2 Assay. For PGE_2 assay, C6 cells were seeded onto 12-well plates at a cell density of 1.0×10^5 cells per well. Two days after cell seeding, cells were subjected to the experiment. Cells were cultured for 18 h in culture medium containing vehicle (0.1% DMSO), γ-mangostin, or NS398, a selective inhibitor of COX-2. The conditioned medium was acidified to pH 4.0 by the addition of 1 N HCl, and PGE_2 was extracted twice with ethyl acetate. After ethyl acetate was evaporated under a stream of N_2 gas, the sample was dissolved in 10 mM Tris-HCl, pH 7.6. PGE_2 was determined by radioimmunoassay, as described previously (Nakatani et al., 2002).

Cell Viability Assay. Cell viability for C6 cells was measured using the MTT method as reported previously (Tagliatela et al., 1997). Cells were seeded onto 96-well plates at a cell density of 1.0×10^4 cells per well and cultured with vehicle or γ-mangostin. Twenty-four hours later, cells were subjected to MTT assay. Product formation was monitored by reading the absorbance at 595 nm using a microplate reader (model 450; Bio-Rad, Hercules, CA).

Semi Quantitative RT-PCR. For RT-PCR, C6 cells were seeded onto six-well plates at a cell density of 2.0×10^5 cells per well. Two days later, cells were pretreated with vehicle or γ-mangostin for 1 h and were incubated subsequently with or without 10 μg/ml LPS for 1 h. The total RNA from cells was prepared by using a total RNA extraction kit. Both the COX-1 and COX-2 mRNA levels were semi-quantitatively assayed using an RT-PCR kit as reported previously (Yang et al., 1998) as follows: The sense primers (5′-CTG CTG AGA AGG GAG TTC AT-3′, 602–621 of rat COX-1 cDNA; and 5′-ACA CTC TAT CAC TGG CAT CC-3′, 1229–1248 of rat COX-2 cDNA) and the antisense primers (5′-GTC ACA CAC ACG GTT ATG CT-3′, 981-1000 of rat COX-1 cDNA; and 5′-GAA GGG ACA CCC TTT CAC AT-3′, 11794-1813 of rat COX-2 cDNA) were complementary to the conserved regions of the cDNAs (Yang et al., 1998). The cDNA fragments were amplified 32 cycles (94°C for 60 s, 62°C for 60 s, and 72°C for 60 s). It was demonstrated that this condition for RT-PCR quantitatively yielded PCR product by our preliminary experiments (data not shown). Glyceraldehyde-3-phosphate dehydrogenase mRNA was used as an internal control for the present semiquantitative RT-PCR. PCR products for COX-1 and COX-2 mRNAs were separated by 2% agarose gel electrophoresis, detected by ethidium bromide staining, and subjected to quantitative analysis using an image scanner (Foto/Eclipse; Fotodyne, Hartland, WI). Furthermore, after purification of the PCR products by electrophoresis and filtration, the nucleotide sequences were determined by the dideoxy nucleotide chain termination method to verify that these PCR products are derived from COX-1 and COX-2 mRNAs.

Immunoblotting. For immunoblotting, C6 cells were seeded onto six-well plates at a cell density of 2.0×10^5 cells per well. Two days after seeding, the cells were incubated with vehicle or γ-mangostin for 1 h at 37°C. After cells were incubated with or without 10 μg/ml LPS for an additional 1 h, the medium was aspirated. The cells were lysed by addition of SDS-PAGE sample buffer (187.5 mM Tris-HCl, 6% SDS, 30% glycerol, and 15% 2-mercaptoethanol, pH 6.8). These protein samples were boiled for 5 min, subjected to SDS-PAGE (8–11% gel), and then transferred electrically onto polyvinylidene difluoride membranes (Immobilon-P; Millipore Corporation, Bedford, MA) by the semidry blotting method. The blots were incubated with 2% bovine serum albumin in Tris-buffered saline containing 0.05% Tween 20 at 25°C for 2 h and incubated with goat anti-COX-1 antibody (0.1 μg/ml), goat anti-COX-2 (0.1 μg/ml), rabbit anti-IκB (0.2 μg/ml), rabbit anti-phospho-IκB (0.2 μg/ml), or rabbit anti-actin (0.2 μg/ml) antibody at 25°C for 2 h. The blots were washed several times and incubated with a 1:1000 to 2000 dilution of alkaline phosphatase-conjugated affinity-purified anti-goat IgG or horseradish peroxide-conjugated affinity-purified anti-rabbit IgG in Tris-buffered saline/Tween 20 containing 2% bovine serum albumin at 4°C overnight. Immunoreactive signals were visualized by incubation of the blots with chemiluminescence assay reagents followed by exposing them to Hyperfilm ECL (Amersham Biosciences).

In Vitro IKK Assay. After 10 min of treatment with 10 μg/ml LPS, C6 cells were washed with phosphate-buffered saline, lysed with ice-cold lysis buffer (2 mM EGTA, 150 mM NaCl, 2 mM dithiothreitol, 1 mM *p*-amidinophenyl methanesulfonyl fluoride hydrochloride, 10 μg/ml leupeptin, 10 μg/ml aprotinin, 1 mM Na_3VO_4, and 10 mM Tris-HCl, pH 7.5), and sonicated to prepare cell extract. IKK proteins were prepared by immunoprecipitation as follows: the cell extract was incubated with 6 μg of anti-IKKα/β antibody at 4°C for 4 h, and the immunocomplex was recovered using protein A Sepharose 4B beads. The IKK protein-bound beads were then washed three times with lysis buffer and were aliquoted to five reaction tubes, including 25 μl of the following kinase reaction mixture: 10 mM $MgCl_2 \cdot 6H_2O$, 0.1 mM Na_3VO_4, 2 mM dithiothreitol, 5 mM β-glycerolphosphate, [γ-^{32}P]ATP, and 25 mM Tris-HCl, pH 7.5. After a 10-min incubation with or without tested concentrations of γ-mangostin at 30°C, 1 μg of IκBα was added as a substrate to each reaction tube, and the reaction mixtures were further incubated for 30 min. The reaction was terminated by the addition of SDS-PAGE sample buffer and fractionated by SDS-PAGE. Phosphorylated IκBα (1–317) was visualized as radioluminogram and quantitatively analyzed with the use of Molecular Imager (GS363; Bio-Rad).

Transient Transfection and Dual Luciferase Assay. C6 cells were plated at a cell density of 3.0×10^4 cells per well on a 24-well plate or 1.2×10^4 cells per well on a 48-well plate. Two days later, the cells were transfected using LipofectAMINE 2000 in serum-free medium according to the manufacturer's recommended method. Cells plated onto 24-well plates were subjected to transfection with 0.475 μg/well pNF-κB-Luc, a firefly luciferase reporter construct containing five repeated NF-κB–responsive elements, or dN-Luc; a reporter plasmid that is deficient in the repeated NF-κB–responsive elements in the pNF-κB-Luc (Hirai et al., 1994). Cells plated onto 48-well plates were also subjected to transfection with 0.4 μg/well of phPES2(−327/+59)-Luc, a firefly luciferase reporter construct containing the human COX-2 gene promoter fragment including NF-κB–responsive element (−223/−214) (Inoue et al., 1995). In addition, to normalize transfection efficiency, C6 cells were cotransfected with 0.025 μg of a *Renilla reniformis* luciferase control vector (phRG-TK). After transfection, cells were cultured in the culture medium for 13 or 20 h and then preincubated with vehicle or γ-mangostin for 3 h. Cells were incubated with or without 1 μg/ml LPS for an additional 13 or 18 h, and then the cells were harvested. Determination of both the firefly and *R. reniformis* luciferase activities was performed using a MiniLumat LB 9506 (Berthold Technologies, Bad Wildbad, Germany) with Dual-Luciferase Reporter Assay System (Promega).

Relative luciferase activity represents the ratio of the activity of firefly luciferase to that of *R. reniformis* luciferase.

Animals. 7-week-old male Wistar rats (weighing 150–170 g) were obtained from Charles River Japan (Yokohama, Japan). All experimental procedures were approved by the Laboratory Animal Care and Use Local Committee of Graduate School of Pharmaceutical Sciences, Tohoku University, and were in accordance with the principles and guidelines on animal care of Tohoku University.

Paw Edema. Paw edema was induced on the left hind paw in each rat by a subplantar injection of 75 μl of sterile saline (0.9% NaCl) containing 1% carrageenan. γ-Mangostin at doses ranging from 1 to 30 mg/kg or the vehicle control (DMSO) was given i.p. 30 min before the carrageenan injection. According to the procedure described previously (Planas et al., 1995), the presence of edema was assessed by measuring the volume of the left hind paw before (V_0) and 5 h after carrageenan injection (V_5). The increase in volume in the inflamed paw was obtained by subtracting the volume measured before the carrageenan injection from the observed value at 5 h and expressed as a percentage: % edema = $[(V_5 - V_0)/V_0] \times 100$.

Data Analysis. IC_{50} values were calculated from nonlinear regression analysis of the data. The data are expressed as the means ± S.E.M., and a significant difference ($P < 0.05$) was analyzed by analysis of variance.

Results

Effect of γ-Mangostin on Spontaneous PGE_2 Release from C6 Cells. Glial cells are an important source of PGs in the CNS (Katsuura et al., 1989). In our earlier report, a short-term (10-min) treatment of C6 cells with γ-mangostin has been demonstrated to reduce A23187 (10 μM)-induced PGE_2 release from the cells (Nakatani et al., 2002). From this finding, we hypothesized that if long-term treatment with γ-mangostin might effectively reduce spontaneous PGE_2 release and/or its production, this compound could be used as a potent anti-inflammatory agent for clinical control of PGE level. Therefore, to first test the possibility, C6 cells were treated with γ-mangostin for 18 h to examine the effect of this compound on the spontaneous release of endogenous PGE_2 from C6 cells. It was revealed that γ-mangostin potently reduced the PGE_2 release in a concentration-dependent manner (Fig. 2A) and that NS398, a selective COX-2 inhibitor, markedly reduced the PGE_2 release at 30 μM (Fig. 2B). γ-Mangostin also had no effect on the cell viability in the concentrations ranging from 0.1 to 30 μM, but at 100 μM, it caused an 80% decrease in the cell viability (data not shown), indicating that this appreciable inhibition of the COX-2–dependent spontaneous PGE_2 release from the cells does not result from a reduction in the cell viability caused by γ-mangostin.

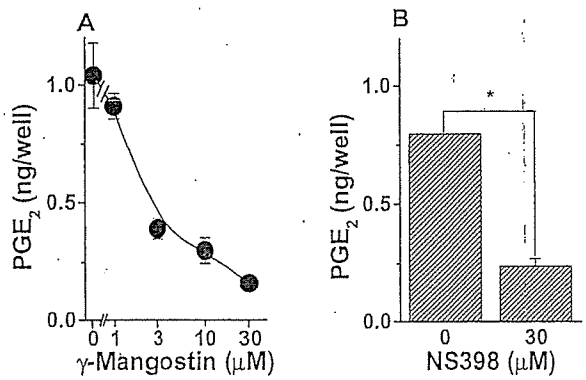

Fig. 2. Concentration-dependent inhibition of endogenous PGE_2 release from C6 cells by γ-mangostin (A) and the effect of NS398 on endogenous PGE_2 release from C6 cells (B). A and B, C6 cells were incubated with the indicated concentrations of γ-mangostin or 30 μM NS398 for 18 h. The released PGE_2 into the culture medium was determined by radioimmunoassay. Each point represents the mean ± S.E.M. ($n = 3$). *, $P < 0.05$ compared with the value for cells treated with 0.1% DMSO (as vehicle control).

Inhibitory Effect of γ-Mangostin on the Expression of Protein and mRNA for COX -2 but Not COX-1 in C6 Cells. COX is a key enzyme for prostaglandin production, because this enzyme is involved in the rate-limiting step in the conversion of AA to prostaglandins (Rosen et al., 1989). Because expression of COX-2 protein and its mRNA are enhanced in response to inflammatory stimuli lasting for several hours (Yamamoto et al., 1995; Inoue and Tanabe, 1998), we next examined whether γ-mangostin affects the expression of COX-1 and COX-2 proteins in C6 cells treated with LPS by immunoblotting. In untreated cells, expressions of COX-1 and COX-2 proteins were detected (Fig. 3, A and B). When treated with LPS, C6 cells showed an increase in protein expression of COX-2 but not COX-1 (Fig. 3, A and B). γ-Mangostin was observed to inhibit this LPS-induced increase in the expression of COX-2 protein in a concentration-dependent manner (Fig. 3B). At 10 μM, this compound also showed a 70% inhibition of the LPS-induced increase in expression of COX-2 protein. In contrast, this compound did not affect the expression of COX-1 protein (Fig. 3A). Furthermore, to examine whether this inhibition of LPS-induced COX-2 protein expression by γ-mangostin results from a reduction in the mRNA level, we analyzed mRNA levels for COX-1 and COX-2 by using RT-PCR. For this assay of mRNA expression of COX-1 and COX-2, an established semiquantitative RT-PCR technique that has been developed recently for determining the regional and temporal profiles of COX-1 and COX-2 mRNA distributions (Yang et al., 1998) was used. Consistent with the results of Western blot analysis described above, γ-mangostin prevented the LPS-induced stimulation of COX-2 mRNA expression in a concentration-dependent manner, with an IC_{50} value of approximately 10 μM in C6 cells, whereas this compound exerted no effect on COX-1 mRNA expression level despite the absence or presence of LPS (Fig. 4, A and B). These results indicate that γ-mangostin may inhibit the expression of COX-2 gene at the transcription level.

Inhibition of NF-κB–Dependent Transcriptional Activation via IKK by γ-Mangostin in C6 Cells. Activation of NF-κB has recently been demonstrated to participate in the induction of expression of COX-2 mRNA by LPS (D'Acquisto et al., 1997) or inflammatory cytokines, including TNF-α (Yamamoto et al., 1995). Therefore, the finding that γ-mangostin prevents the LPS-induced augmentation of expression of COX-2 mRNA in C6 cells raises the possibility that this reduction in expression of COX-2 mRNA by γ-mangostin is the consequence of an inhibition of LPS-induced activation of COX-2 gene transcription through the NF-κB/IκB system. It was thus examined whether γ-mangostin directly influences IKK activity, which phosphorylates IκB protein, using an in vitro IKK assay system. As shown in Fig. 5, γ-mangostin exhibited a concentration-dependent inhibition of the IKK activity with an IC_{50} of approximately 10 μM in vitro, demonstrating that this compound directly inhibits the IKK activity. Next, the phosphorylation and accumulation of IκBα in C6 cells treated with LPS in the absence or presence

of γ-mangostin was analyzed by Western blotting. γ-Mangostin was shown to inhibit the LPS-induced IκB phosphorylation in a concentration-dependent manner and cause an 80% inhibition of the LPS-induced IκB phosphorylation at 10 μM (Fig. 6A). When assayed by Western blotting, it was also shown that γ-mangostin inhibited LPS-induced IκB degradation in a concentration-dependent manner, with an IC_{50} of 10 μM (Fig. 6B). It has been well-documented that proteolytic degradation of IκB is involved in an activation of NF-κB. Thus, to further determine whether treatment with γ-mangostin actually inhibits NF-κB–dependent transcription activity in LPS-induced C6 cells, we conducted transient transfection of C6 cells with pNFκB-Luc, an NF-κB–dependent luciferase reporter plasmid, or dN-Luc, the NF-κB–responsive element-deficient pNFκB-Luc, and assayed the luciferase activity in C6 cells treated with vehicle or γ-mangostin in the absence or presence of LPS. As shown in Fig. 7A, LPS increased the luciferase activity in C6 cells transfected with pNFκB-Luc, whereas LPS-treated cells did not show such an increase in the luciferase activity when transfected with dN-Luc, demonstrating that the LPS-induced stimulation of luciferase activity is NF-κB–dependent. Furthermore, it was shown that at 10 μM, γ-mangostin inhibited the NF-κB–dependent transcriptional activation induced by LPS (Fig. 7A). γ-Mangostin also reduced LPS-induced augmentation of the luciferase activity in C6 cells transfected with phPES2 (−327/+59)-Luc, a human COX-2 reporter gene containing an NF-κB–responsive element, at 30 μM (Fig. 7B).

Inhibition of Rat Carrageenan-Induced Paw Edema by γ-Mangostin. To evaluate the anti-inflammatory activity of γ-mangostin in vivo, rat carrageenan-induced hind paw edema was used as an acute model of inflammation. γ-Mangostin exhibited a concentration-dependent inhibition of the edema and produced remissions of the inflammatory reaction at the doses of 10 and 30 mg/kg, demonstrating that this compound has an anti-inflammatory activity in vivo (Fig. 8).

Discussion

The fruit hull of mangosteen, *G. mangostana*, has been widely used as an anti-inflammatory medicine in Southeast Asia for many years (Mahabusarakam et al., 1987). γ-Mangostin is one of the main constituents contained in the fruit hull of mangosteen. In the present study, we revealed that long-term treatment with γ-mangostin effectively reduced spontaneous PGE_2 release from C6 rat glioma cells, which was shown to be appreciably inhibited by NS398, a selective COX-2 inhibitor, without affecting the cell viability, and that this natural product, like aspirin (Yin et al., 1999), inhibited IKK activity in vitro and consistently reduced LPS-induced NF-κB–dependent transcriptional activation responsible for COX-2 gene transcription, which resulted in the decrease in LPS-induced COX-2 gene expression in C6 cells. Moreover, as expected, γ-mangostin was shown to prevent rat carrageenan-induced hind paw edema used as an acute model of inflammation. We thus suggest that γ-mangostin serves as not only a potent inhibitor of the release of an inflammatory chemical mediator, PGE_2, but also a new inhibitor of COX-2 gene activation and, as a result, acts as an anti-inflammatory agent in vivo.

In this study, we observed that both COX-1 and COX-2 proteins and their mRNA were expressed in the untreated cells. More than 60% of spontaneous PGE_2 release from C6 glioma cells was inhibited by an 18-h treatment with 30 μM NS398, demonstrating that COX-2 mainly contributes to this spontaneous PGE_2 release. In our earlier study, it was demonstrated that suppression of A23187-induced PGE_2 release by γ-mangostin results from its direct inhibition of the COX-1

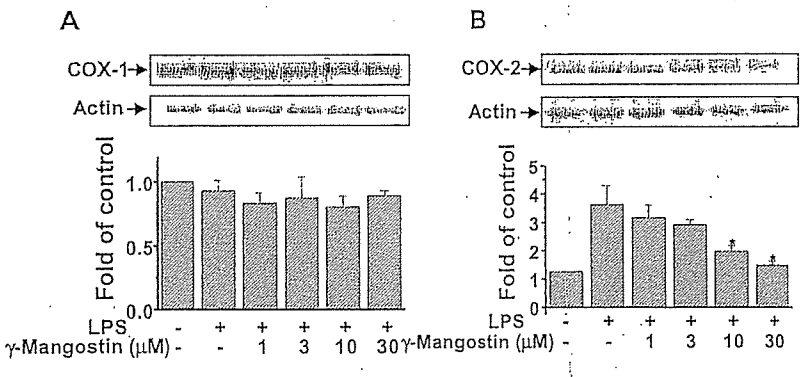

Fig. 3. Decreasing effect of γ-mangostin on the expression of COX-1 (A) and COX -2 (B) proteins as assayed by immunoblotting. After preincubation with the indicated concentrations of γ-mangostin or without this compound for 1 h, cells were incubated in the absence or presence of 10 μg/ml of LPS for 1 h. Shown are representative expression patterns from three independent experiments (top). The densitometric data on the expression of COX-1 and COX -2 proteins (bottom) were calculated as the fold increase of the value for untreated cells. Each column represents the mean ± S.E.M. (n = 3). *, $P < 0.05$ compared with the value for cells treated with 0.1% DMSO (as vehicle control). Actin protein was used as the loading control.

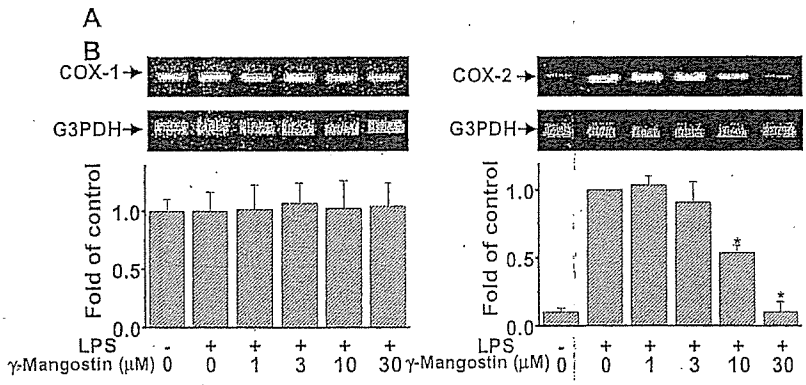

Fig. 4. Decreasing effects of γ-mangostin on COX-1 (A) and COX-2 (B) mRNA expression in C6 cells as measured by RT-PCR. Cells were preincubated with the indicated concentrations of γ-mangostin or without this compound for 1 h and thereafter were incubated in the absence or presence of 10 μg/ml LPS for 1 h. Total RNA from C6 cells was used as a template for cDNA synthesis and then subjected to PCR as described under *Materials and Methods*. Glyceraldehyde-3-phosphate dehydrogenase mRNA was used as the loading control. Shown are representative expression patterns from three independent experiments (top). The densitometric data on COX-1 and COX-2 mRNA expression (bottom) are calculated as the fold increase of the value for cells not treated with γ-mangostin. Each point represents the mean ± S.E.M. (n = 3). *, $P < 0.05$ compared with the value for cells treated with 0.1% DMSO (as vehicle control).

and COX-2 activities in C6 cells, like aspirin and sodium salicylate, nonsteroidal anti-inflammatory drugs (NSAIDs) (Nakatani et al., 2002). COX is the rate-limiting enzyme in the conversion of AA to prostanoids (Rosen et al., 1989). Therefore, we suggest that a marked reduction in the spontaneous PGE_2 release from C6 glioma cells by long-term treatment with γ-mangostin mainly results from a direct inhibition of the COX-2 activity by this natural compound.

Activation of COX-2 gene transcription is mediated by several *cis*-acting promoter elements that respond to multiple intracellular signaling pathways (Mestre et al., 2001); that is, the specific factors involved in the activation of COX-2 gene transcription depend on the cell types and the stimuli. In C6 cells, LPS was observed to stimulate NF-κB– but not activator protein-1–, cAMP-responsive element-, and glucocorticoid response element-dependent transcription (K. Aoki, T. Yamakuni, K. Nakatani, N. Kondo, H. Oku, K. Ishiguro, and Y. Ohizumi, unpublished data). Furthermore, as described above, it was found that LPS induced an increase in the expression of protein and mRNA for COX-2 but not COX-1 in C6 Cells, and that γ-mangostin inhibited the LPS-induced increase in the expression of protein and mRNA for COX-2 in a concentration-dependent manner. The most important finding of the present study is that γ-mangostin has a pharmacological activity of preventing stimulation of NF-κB, a central mediator of inflammation by LPS, by directly inhibiting IKK activity, which resulted in a decrease in LPS-induced phosphorylation and degradation of IκB. This finding raises the possibility that γ-mangostin inhibits IKK activity in vivo to decrease the LPS-induced augmentation of COX-2 gene expression. It was indeed observed that γ-mangostin produced remission of the inflammatory reaction in a concentration-dependent manner, when assayed in an in vivo model of inflammation. It has been shown thus far that aspirin and sodium salicylate inhibit NF-κB activation and IKKβ kinase activity with IC_{50} values of 30 to 50 μM in vitro (Yin et al., 1999) and that these agents suppress LPS-inducible COX-2 gene transcription (Xu et al., 1999). As evaluated using an in vitro assay system, the inhibition of IKK kinase activity by γ-mangostin showed an IC_{50} of approximately 10 μM, although γ-mangostin and these NSAIDs exhibited no chemical structure similarities. On the other hand, antioxidants such as pyrrolidinedithiocarbamate and *N*-acetylcysteine have been reported to inhibit IKK activation in endothelial cells (Spiecker et al., 1998). Taken together, these pharmacological characteristics of this natural product thus provide a plausible explanation for the anti-inflammatory action of the fruit hull of mangosteen, although the precise dual mechanisms of inhibitory actions of γ-mangostin remain to be elucidated.

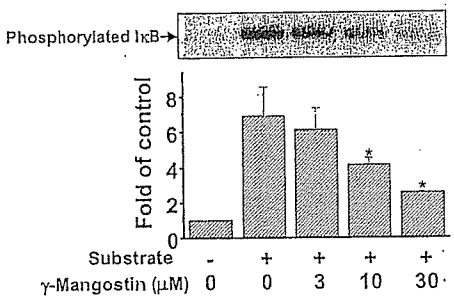

Fig. 5. Concentration-dependent inhibitory effect of γ-mangostin on IKK activity. C6 cells were harvested, lysed, and immunoprecipitated with anti-IKKα/β antibody. The kinase assay was carried out in 25 μl of kinase buffer containing 5 μM ATP, 10 μCi [γ-^{32}P]ATP (5000 Ci/mmol), and 1 μg IκBα (1–317) as a substrate and incubated with the indicated concentrations of γ-mangostin at 25°C for 30 min. The samples were subjected to SDS-PAGE (11% gel). At the top is a representative radioluminogram detected by using a molecular imager (GS363; Bio-Rad). At the bottom, data obtained by densitometry are shown. The results are shown as the fold increase from the value for a sample excluding the substrate and γ-mangostin (0.1% DMSO alone). Each column represents the mean ± S.E.M. (n = 3). *, $P < 0.05$ compared with the value for the sample containing the substrate but not γ-mangostin (as vehicle control).

Astrocytes are a known important, although not the only, source of PGE_2 in the CNS (Katsuura et al., 1989). Their ability to produce PGE_2 upon stimulation with IL-1β, TNF-α, or LPS has been extensively documented (Fontana et al., 1982; Mollace et al., 1998; Molina-Holgado et al., 2000). The increase in PGE_2 levels has been observed in some diseases, including AIDS-associated dementia (Minghetti et al., 1998). Expression of COX-2 in astrocytes has been demonstrated in vitro as well as in vivo. COX-2 expression has been detected in astrocytes of patients suffering from amyotrophic lateral sclerosis (Almer et al., 2001) as well as in astrocytes surrounding the plaques in a mouse model of AD (Matsuoka et al., 2001). Furthermore, the level of astrocytic COX-2 expression in brain tumors was shown to be among the best indicator of tumor progression and severity (Shono et al., 2001). In addition, increased COX-2 expression by tissue macrophages is responsible for the accumulation of large amounts of PGE_2 in local tissues (Smith et al., 2000). Secreted PGE_2 promotes inflammation by increasing vascular permeability and vasodilation and by directing cell migration into the site of inflammation through the induction of inflammatory cytokines (Muraoka et al., 1999). Therefore, the control of PGE_2 production is a critical step in clinically regulating inflammatory reactions during bacterial infection and tissue injury. From the fact that γ-mangostin inhibits stimulation of

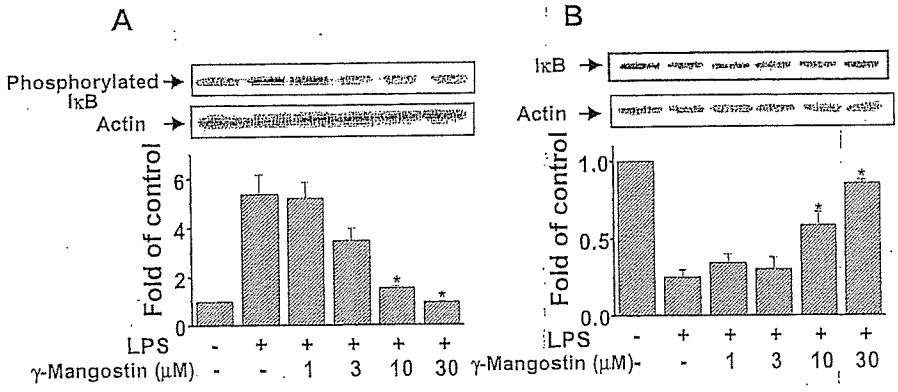

Fig. 6. Concentration-dependent inhibition of LPS-induced phosphorylation (A) and degradation (B) of IκB protein by γ-mangostin in C6 cells. Cells were preincubated with the indicated concentrations of γ-mangostin or without this compound for 1 h and thereafter were incubated in the absence or presence of 10 μg/ml LPS for 0.5 h (A) and 1 h (B). Shown are representative phosphorylation and degradation patterns from three independent experiments (top). The densitometric data on the phosphorylation and degradation of IκB protein (bottom) were calculated as the fold increase of the value for untreated cells. Each column represents the mean ± S.E.M. (n = 3). *, $P < 0.05$ compared with the value for cells treated with 0.1% DMSO (as vehicle). Actin protein was used as the loading control.